

## Genomics–Metabolomics Profiling Disclosed Marine *Vibrio spartinae* 3.6 as a Producer of a New Branched Side Chain Prodigiosin

Giovanni Andrea Vitale, Martina Sciarretta, Fortunato Palma Esposito, Grant Garren January, Marianna Giaccio, Boyke Bunk, Cathrin Spröer, Felizitas Bajerski, Deborah Power, Carmen Festa, Maria Chiara Monti, Maria Valeria D’Auria,\* and Donatella de Pascale\*



Cite This: <https://dx.doi.org/10.1021/acs.jnatprod.9b01159>



Read Online

ACCESS |



Metrics & More

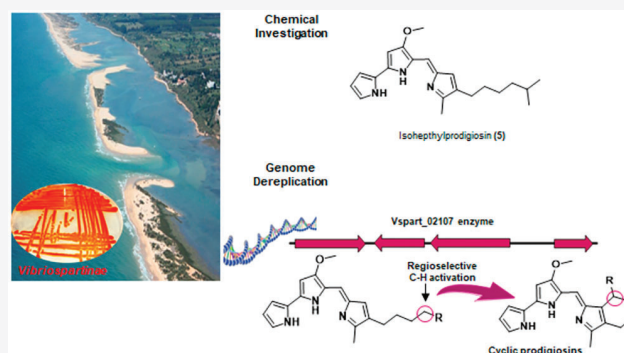


Article Recommendations



Supporting Information

**ABSTRACT:** A wide range of prescreening tests for antimicrobial activity of 59 bacterial isolates from sediments of Ria Formosa Lagoon (Algarve, Portugal) disclosed *Vibrio spartinae* 3.6 as the most active antibacterial producing strain. This bacterial strain, which has not previously been submitted for chemical profiling, was subjected to *de novo* whole genome sequencing, which aided in the discovery and elucidation of a prodigiosin biosynthetic gene cluster that was predicted by the bioinformatic tool KEGG BlastKoala. Comparative genomics led to the identification of a new membrane di-iron oxygenase-like enzyme, annotated as Vspart\_02107, which is likely to be involved in the biosynthesis of cycloprodigiosin and analogues. The combined genomics–metabolomics profiling of the strain led to the isolation and identification of one new branched-chain prodigiosin (**5**) and to the detection of two new cyclic forms. Furthermore, the evaluation of the minimum inhibitory concentrations disclosed the major prodigiosin as very effective against multi-drug-resistant pathogens including *Stenotrophomonas maltophilia*, a clinical isolate of *Listeria monocytogenes*, as well as some human pathogens reported by the World Health Organization as prioritized targets.



The family of tripyrrole red pigments, prodiginines, have attracted considerable research interest over the last few decades due to their wide range of bioactivities, which include antibacterial, antifungal, antiprotozoal, and antimalarial actions.<sup>1</sup> In particular, the immunosuppressant action of natural or synthetic prodiginines<sup>2</sup> has been well investigated, and they have a distinctly different immunomodulatory mechanism than that of cyclosporine. Moreover, they are effective pro-apoptotic agents at nontoxic concentrations.<sup>3–6</sup> Extensive medicinal chemistry optimization of the natural molecules led to the development of a synthetic derivative, obatoclax mesylate (GX15-070), which has been shown to modulate autophagy and has been used in multiple phase I and II combinatorial cancer chemotherapeutics.<sup>7,8</sup> Prodiginines owe their name to their connection with an important miracle of the Christian church, i.e., “The Miracle of Bolsena” (1263): A priest fighting against his decreasing faith received a “prodigious” sign during a Mass when blood started dripping from the holy bread. A few centuries later, the Miracle of Bolsena was explained by the fermentation of the bacterium *Serratia marcescens* on bread, associated with the production of a red pigment.<sup>9,10</sup> Prodigiosin production was first reported for *Serratia marcescens* and then subsequently identified in a variety of terrestrial and marine Gram-positive and Gram-negative

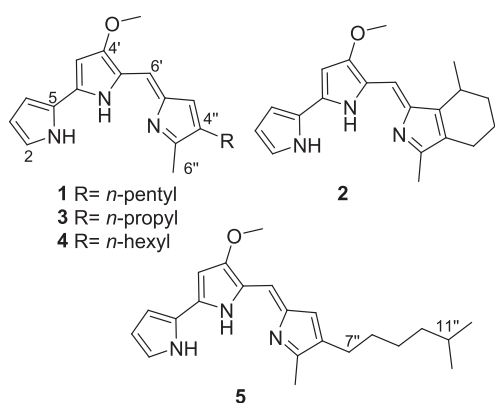
microorganisms including *Pseudomonas magnesiiorubra*, *Hahella chejuensis*, *Zooshikella rubidus*, *Streptomyces* spp., and *Nocardia* spp.<sup>11–14</sup> Other bacteria such as *Pseudoalteromonas rubra*, *Vibrio gazogenes*, and *Zooshikella rubidus* are able to synthesize cycloprodigiosin in addition to prodigiosin.<sup>13,15,16</sup> Despite the large number of natural producers, there is only minor chemical diversity associated with natural prodiginines. They fall into two broad groups: (1) linear alkyl chain derivatives exemplified by prodigiosin (1) and undecylprodigiosin and (2) cyclic derivatives of prodiginines, such as cycloprodigiosin (2) and streptorubin B.<sup>2,9,17</sup> The ubiquitous presence of prodiginines in phylogenetically distant bacterial strains seems to indicate a physiological role of these pigments, although the actual role, as for many natural products, is still unclear. The antimicrobial activity of purified prodiginines has been reported in relation to common Gram-positive and Gram-negative bacterial strains such as *Staphylococcus aureus*,

Received: November 21, 2019

*Escherichia coli*, and *Bacillus subtilis*.<sup>1,18,19</sup> Analysis of the structure–function relationship of linear and cyclic prodiginines suggests the latter have an enhanced conformational bias toward the interaction with a biological target, which in some cases is associated with increased activity, although no scientific consensus yet exists.<sup>15</sup>

In the context of screening for bioactive metabolites from marine microorganisms, herein, we report on the chemical and biological investigation of a new prodiginosin producer, *Vibrio spartinae*, recently described as a new bacterial species.<sup>20</sup> The bacterium was selected among 59 isolated bacteria from sediments collected in the Ria Formosa lagoon (Algarve, Portugal), for their powerful inhibitory activity exhibited during prescreening for antimicrobial activity against four human pathogens. The study resulted in an almost completely annotated genome of *V. spartinae*, the isolation of both prodiginosin and cycloprodiginosin as major compounds, and the isolation of the first example of a branched-chain prodiginosin, biosynthesized by prodiginosin (*pig*) biosynthetic gene cluster (BGC). Furthermore, through an integrated approach that involved HR-MS<sup>n</sup> experiments and comparative genomics, the strain was shown to express an alkylglycerol monoxygenase-like enzyme encoded by *Vspart\_02107*, which is a homologue of PRUB680, recently reported from *P. rubra*. The enzyme likely catalyzes the final cyclization step from prodiginosin to cycloprodiginosin, and it appears to regioselectively catalyze the cyclization of all the linear prodiginosins to their corresponding cyclic derivatives.

A wide-range screening for antimicrobial activity of the isolated molecules revealed that the major prodiginosin is particularly effective against *Listeria monocytogenes*, the causative agent of listeriosis,<sup>21</sup> and *Stenotrophomonas maltophilia*, one of the leading drug-resistant hospital-associated pathogens.<sup>22</sup>



## RESULTS AND DISCUSSION

**Selection, Identification, and Genome Characterization of the *Vibrio spartinae* 3.6.** Recently, in the framework of the EMBRIC Transnational Access program (<http://www.embric.eu/projects/embriceuropean-marine-biological-research-infrastructure-cluster>), a total of 24 sediments (Supporting Information, Table S1) were collected from four different points (six replicates each) located in the Ria Formosa lagoon (Algarve, Portugal). The natural park of Ria Formosa is a complex of shallow water and lagoons, known for high fluctuations in tide and high salinity,<sup>23</sup> which makes this environment suitable for the isolation of interesting microorganisms. From these sediments, 59 bacterial strains were

isolated and subjected to prescreening for antimicrobial activity on agar plates. The representative pathogenic strains included in the screening were three Gram-negative strains (*Pseudomonas aeruginosa* PAO1, *Escherichia coli* ATCC 25922, and *Acinetobacter baumannii* 13) and one Gram-positive strain (*Staphylococcus aureus* ATCC 6538P). Out of the five active bacteria identified from sediments, the pink bacterial strain labeled 3.6 (isolated from sediment 7B) showed a pronounced lytic halo toward all of the strains with the exception of *P. aeruginosa* (Table S2) and was therefore selected for further investigation. The complete 16S rRNA gene was extracted from the fully assembled genome of *V. spartinae* 3.6 and was compared to the nonredundant (nr) database at NCBI limiting the search to type material. They shared 99.25% similarity to *V. spartinae* SMJ21<sup>T</sup> with SMJ21<sup>T</sup>=CECT 9026<sup>T</sup>=LMG 29723<sup>T</sup>.<sup>20</sup> Whole genome sequencing (WGS) of *V. spartinae* 3.6 yielded a genome of 5.0 Mbp distributed between two bacterial chromosomes of 3.8 and 1.2 Mbp, respectively, with a GC content of 45.5%. No further plasmids were detected. Prokka predicted 4320 protein-coding sequences, 90 tRNA and 25 rRNA genes (Table 1).

**Table 1. Genome Attributes of *De Novo* WGS of *Vibrio spartinae* 3.6**

attribute	value
genome size (bp)	5 010 010
DNA G+C content (bp)	45.5
number of contiguous sequences	2
extrachromosomal elements (plasmids)	0
total genes	4520
coding sequences (CDS)	4320
signal peptides	318
tRNA genes	90
rRNA genes (operons)	25 (8)
miscellaneous RNA	84
tmRNA	1
repeat regions	17

To taxonomically delineate *V. spartinae* 3.6, pairwise comparisons were conducted using the Type Strain Genome Server (TYGS), which showed 93% digital DNA–DNA hybridization (dDDH) to *V. spartinae* SMJ21<sup>T</sup>, the closest related type strain to *V. spartinae* 3.6. The probability that this value is correct was confirmed by the confidence interval that was between 91% and 94% by linear regression. The threshold for correct taxonomic assignment using dDDH is  $\geq 70\%$  for species classification. Therefore, based on these results it was concluded with a high degree of confidence that isolate 3.6 can be correctly assigned to *V. spartinae*.<sup>24</sup> Here, we see the user strain “*Vibrio*” is contained within the same species cluster as the type strain *V. spartinae* SMJ21<sup>T</sup>=CECT 9026<sup>T</sup>=LMG 29723<sup>T</sup> (Figure 1).

Primary metabolism of the isolate was reconstructed from genome sequence data (translated amino acids) using KEGG BlastKoala.<sup>25</sup> These data were then used to predict (*in silico*) the biosynthetic pathway of prodiginosin (Figure S1). Thereafter, we confirmed the BGC of *V. spartinae* 3.6 by comparative genomics using the prodiginosin BGC from *S. marcescens* (GenBank accession number AJ833001.1) as the reference. Within the genome of *V. spartinae* 3.6 we discovered the presence of *pigB*–*pigN* as a complete gene cluster, while C-terminal similarity to *pigA* can be found within *Vspart\_03968*

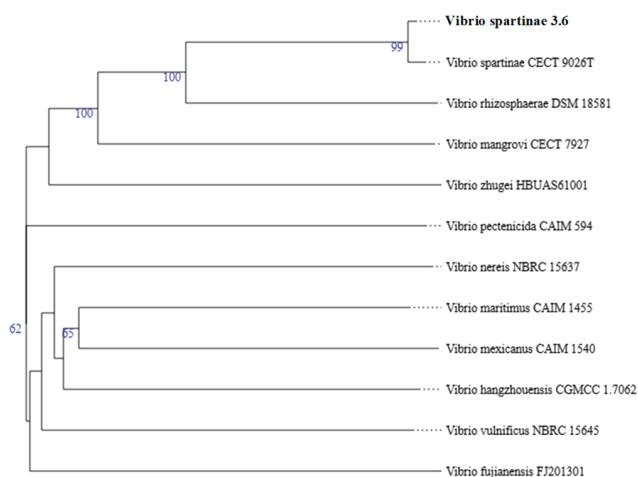


**Figure 1.** Genome BLAST distance phylogeny (GBDP) by WGS data of *V. spartinae* 3.6. The phylogenetic tree has been inferred from GBDP distances calculated from genome sequences within the Type Strain genome server ([tygs.dsmz.de](http://tygs.dsmz.de)). The numbers below the branches are GBDP pseudobootstrap support values from 100 replications, with an average branch support of 63.6%. The tree was rooted at the midpoint.

located separately on the second chromosome (Figure S2), but this might also be a result of its high sequence similarity to the Acyl-CoA dehydrogenase Adh.

**Chemical Identification of Prodigiosins.** *V. spartinae* 3.6 was grown in 200 mL of MB mod liquid media at 20 °C for 3 days, and the intracellular and extracellular extracts were mixed, dissolved in mass grade MeOH at a concentration of 1 mg/mL, and analyzed using LC-HRMS in positive mode.

The total ion chromatogram (TIC) shown in Figure 2 highlights the presence of two major peaks, peak B and peak D, respectively, with  $[M + H]^+$  of 322.1914 and 324.2071, which

are compatible with the pink pigment prodigiosin (1), first isolated from *Serratia marcescens*<sup>2</sup> and cycloprodigiosin (2), its cyclic homologue, respectively. The remaining peaks, visible in the LC trace—A, C, E, F, and G—showed protonated molecules  $[M + H]^+$  at  $m/z$  296.1756, 336.2070, 350.2227, 338.2227, and 352.2383, respectively.

The peaks A, F, and G showed molecular weights corresponding to prodigiosin derivatives with C3-, C6-, and C7-alkyl side chains at the 4'' position. Prodigiosin analogues with different alkyl side chains have already been reported in *Zooshikella rubidus*,<sup>13</sup> *Pseudoalteromonas rubra*,<sup>26</sup> and other *Vibrio* spp.,<sup>15</sup> although in some cases the structures were only deduced on the basis of ESIMS data. On the other hand, the molecular weights of peaks C and E indicated one additional unsaturation degree with respect to the peaks F and G.

In order to confirm the results of the LC-HRMS chemical profiling and to assess the antimicrobial activity of the pure prodigiosin components, a large-scale optimized fermentation was established in the same liquid media, and an extract of about 600 mg was prepared and was subjected to repeated solvent partitioning. A preliminary purification by HPLC fractionation gave the major components, prodigiosin (1) and cycloprodigiosin (2), and three enriched fractions, which were further purified by HPLC to isolate the compounds in peaks A, F, and G. Unfortunately, due to their low abundance and to the presence of some UV-undetectable contaminations, it was impossible to obtain sufficiently purified compounds from peaks C and E for NMR characterization. NMR analysis of the compounds in peaks A, B, D, and F (Table S4) confirmed their identity as 4''-propylprodigiosin (3), cycloprodigiosin (2), prodigiosin (1), and 4''-hexylprodigiosin (4).<sup>15</sup>

The absolute configuration of naturally occurring cycloprodigiosin remained unknown for a long time. Only recently, the enantioselective total synthesis of both enantiomers and a combination of X-ray and chiral-phase HPLC analyses allowed

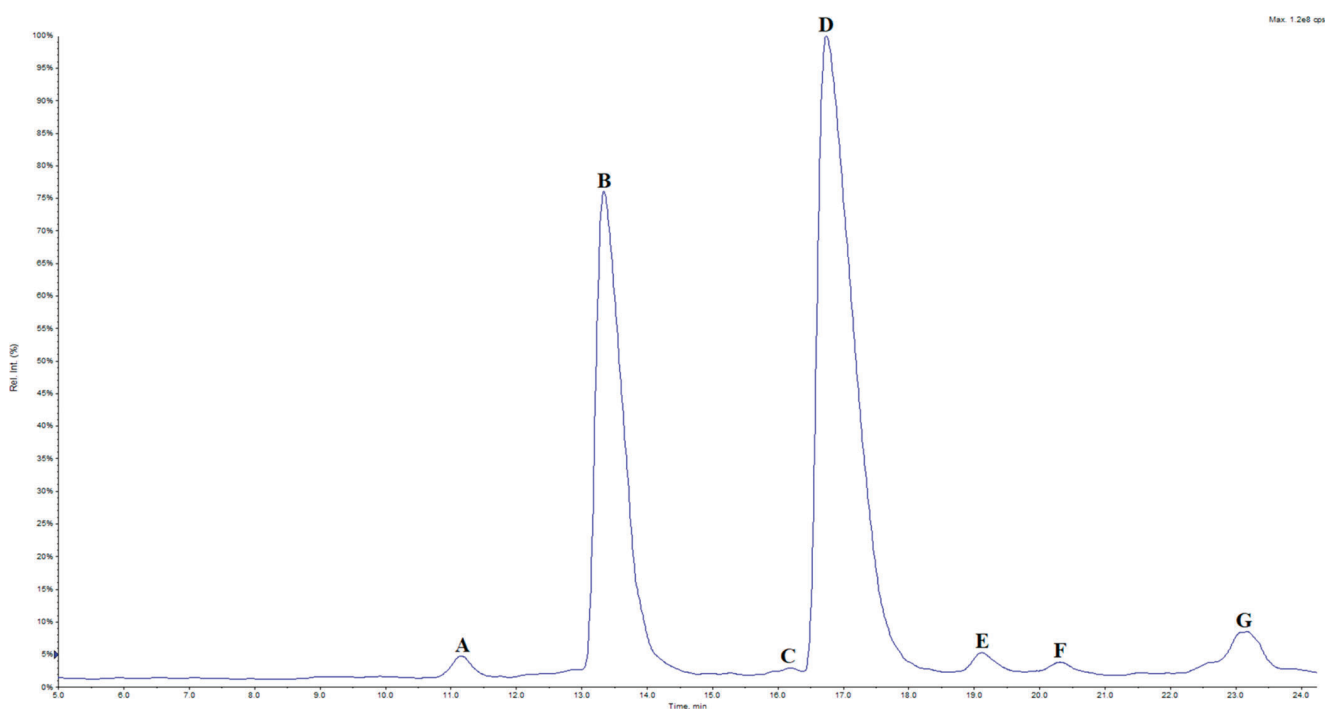


**Figure 2.** ESI positive mode total ion chromatogram (TIC) of the *Vibrio spartinae* 3.6 MeOH extract.

for the determination of the natural cycloprodiginosin from *P. rubra* ATCC 29570, as a scalemic mixture occurring in an enantiomeric ratio of 83:17 (R)/(S).<sup>27</sup>

Accordingly, when we subjected cycloprodiginosin (**2**) from *V. spartinae* 3.6 to chiral-phase HPLC analysis, a comparable ratio was observed (Figure S4).

The molecular formula of compound **5** was deduced as C<sub>22</sub>H<sub>29</sub>N<sub>3</sub>O based on the protonated molecule [M + H]<sup>+</sup> at *m/z* 352.2383 in conjunction with <sup>1</sup>H and <sup>13</sup>C spectroscopic data. The HRESI MS/MS spectrum showed the fragment ion at *m/z* 252.1130, due to the loss of the side chain, which is a fingerprint of the linear prodiginosins, suggesting a core prodiginine structure with a seven-carbon side chain.<sup>28</sup> The <sup>1</sup>H and <sup>13</sup>C NMR analysis gave a total match for the signals relative to the prodiginosene nucleus (Table 2), and this was

**Table 2.** <sup>1</sup>H (400 MHz) and <sup>13</sup>C (125 MHz) NMR Assignment of Isoheptylprodiginosin, **5** (CDCl<sub>3</sub>)<sup>a</sup>

isoheptylprodiginosin ( <b>5</b> ) <sup>b</sup>				
position	δ <sub>C</sub> , type	δ <sub>H</sub> (J in Hz)	COSY	HMBC <sup>c</sup>
NH1		12.4, br s	2, 3, 4	
2	127.2, CH	7.25, br s	NH1, 3	3, 4, 5
3	111.9, CH	6.36, br s	NH1, 2, 4	5
4	117.4, CH	6.92, br s	NH1, 3	5
5	121.9, C			
NH1'		12.56 <sup>d</sup>	3'	
2'	147.5, C			
3'	92.9, CH	6.08, s	NH1'	2', 5'
O-Me	58.7	4.01, s		4'
4'	166.3, C			
5'	121.8, C			
6'	116.1, CH	6.95, s	NH1'	4', 3"
NH1" <sup>b</sup>		12.58 <sup>d</sup>	3"	
2"	126.4, C			
3"	128.6, CH	6.67, m	NH1", 6", 7"	2", 5"
4"	128.9, C			
5"	146.9, C			
6"	12.4, CH <sub>3</sub>	2.52, s	3"	4", 5"
7"	25.3, CH <sub>2</sub>	2.41, t (7.5 Hz)	3", 8"	4", 5", 8"
8"	30.1, CH <sub>2</sub>	1.52 <sup>d</sup>	7", 9"	
9"	26.9, CH <sub>2</sub>	1.31, m	8", 10"	
10"	38.8, CH <sub>2</sub>	1.19, m	9", 11"	
11"	27.8, CH	1.50 <sup>d</sup>	12", 13"	
12"				
13"	22.4, CH <sub>3</sub>	0.88, d (6.6 Hz)	11"	11", 10"

<sup>a</sup>NMR solvent was established for comparative purpose with literature data and to detect exchangeable protons, despite low solubility observed for the compound in this solvent. <sup>b</sup>HPLC conditions furnished pure compound in the protonated form. <sup>c</sup>HMBC correlations are from the proton(s) stated to the indicated carbon. <sup>d</sup>Overlapped with other signals.

confirmed by 2D NMR analysis. However, in the <sup>1</sup>H NMR spectrum, the usual terminal methyl triplet signal was replaced by a doublet at δ<sub>H</sub> 0.88 integrating for six protons. This finding, together with the relative corresponding <sup>13</sup>C NMR chemical shift value (δ<sub>C</sub> 22.4) as determined by the analysis of the HSQC spectrum, was indicative of an isopropyl terminal subunit. The assignment of the chemical shift values of the seven carbon branched 4"-methylhexyl side chain was straightforward and established by the analysis of 2D COSY,

HSQC, and HMBC spectra. For the new compound **5** we propose the name isoheptylprodiginosin.

There are other examples of branched side chain derivatives in the prodiginine pigment family, i.e., cyclic prodiginosins R1 and R2 and linear 11-methyldodecylprodiginine.<sup>29,30</sup> However, the biosynthesis of the above compounds, isolated from *Streptomyces griseoviridis*, involved the *red* (23 genes) gene cluster, characteristic of Gram-positive *Streptomyces* spp.,<sup>2</sup> which is distinct from the *pig* gene cluster (17 genes) in the Gram-negative *Serratia* spp., responsible for prodiginosin biosynthesis. The isolation of isoheptylprodiginosin (**5**) from the Gram-negative *V. spartinae* 3.6 represents the first report of a branched-chain prodiginosin arising from the *pig* gene cluster. In particular, in the *red* gene cluster, the constitution of an alkyl side chain on the right monopyrrole ring is related to the substrate loading selectivity of RedP, and the replacement by plasmid-based bioengineering of the RedP's function with a *Streptomyces* FAS FabH<sup>31</sup> was reported to produce branched-chain prodiginines related to undecylprodiginosins. On the other hand, in the *pig* gene cluster, the length and the constitution of the side chain on the right methyl-alkyl-pyrrole subunit is influenced by the loading of different 2-alkenoyl CoAs by the thiamine diphosphate-dependent *pigD*.<sup>32</sup> Probably, the *pigD* homologue in *V. spartinae* 3.6 *Vspart\_01681* is able to load 8-methyl-2-nonenoylCoA, which in turn could be derived from the metabolism of an iso-fatty acid arising from a branched-chain starter unit (Figure 3).

***Vibrio spartinae* 3.6 Is Able to Regiospecifically Catalyze Linear Prodiginosin Cyclization.** Thus far, two unclustered biosynthetic genes have been reported to be responsible for the final transformation of prodiginine linear precursors to their cyclic congeners. In *Streptomyces* spp. the cyclization reaction used to produce cyclic prodiginine derivatives, such as streptorubin B, metacycloprodiginosin, marineosin, prodiginosin R1, and roseophilin, occurs through the action of enzymes belonging to the family of Rieske oxygenases, which are exemplified by REDG in *Streptomyces coelicolor*.<sup>33,34</sup> On the other hand, recent studies on the Gram-negative *P. rubra* DSM 6842 = ATCC 29570 genome<sup>16</sup> disclosed a completely unrelated alkylglycerol monooxygenase-like enzyme, di-iron oxygenase encoded by PRUB680, which was responsible for the regiospecific C10"-H activation and cyclization of prodiginosin to cycloprodiginosin in *P. rubra*.<sup>16</sup> Interestingly, when the whole genome sequence of *V. spartinae* 3.6 was compared to REDG and PRUB680, no match was found with REDG. However, comparison with PRUB680 (GenBank accession no. ERG47138.1) identified a gene, *Vspart\_02107* (Figure 4), that shared 81% similarity at the amino acid level with PRUB680 based on BLASTP analysis. Moreover, the fatty acid hydroxylase encoded by this gene displayed the conserved histidine motif, which is known to be essential for both iron binding and catalysis,<sup>35,36</sup> and a similar transmembrane topology (Figure S3). Again, the observed incomplete enantioselectivity in the carbocyclization process is another common feature.

A careful analysis of the HR-MSMS fragmentation pattern of the minor prodiginosin-like compounds, which featured one additional unsaturation degree (peaks C and E in Figure 2), revealed the absence of the key fragment *m/z* 252.1131 due to the loss of the alkyl side chain at C-4", a common feature of all linear prodiginosins; additionally, the common fragments C and D+B suggested a common six-membered cycloprodiginosin-like

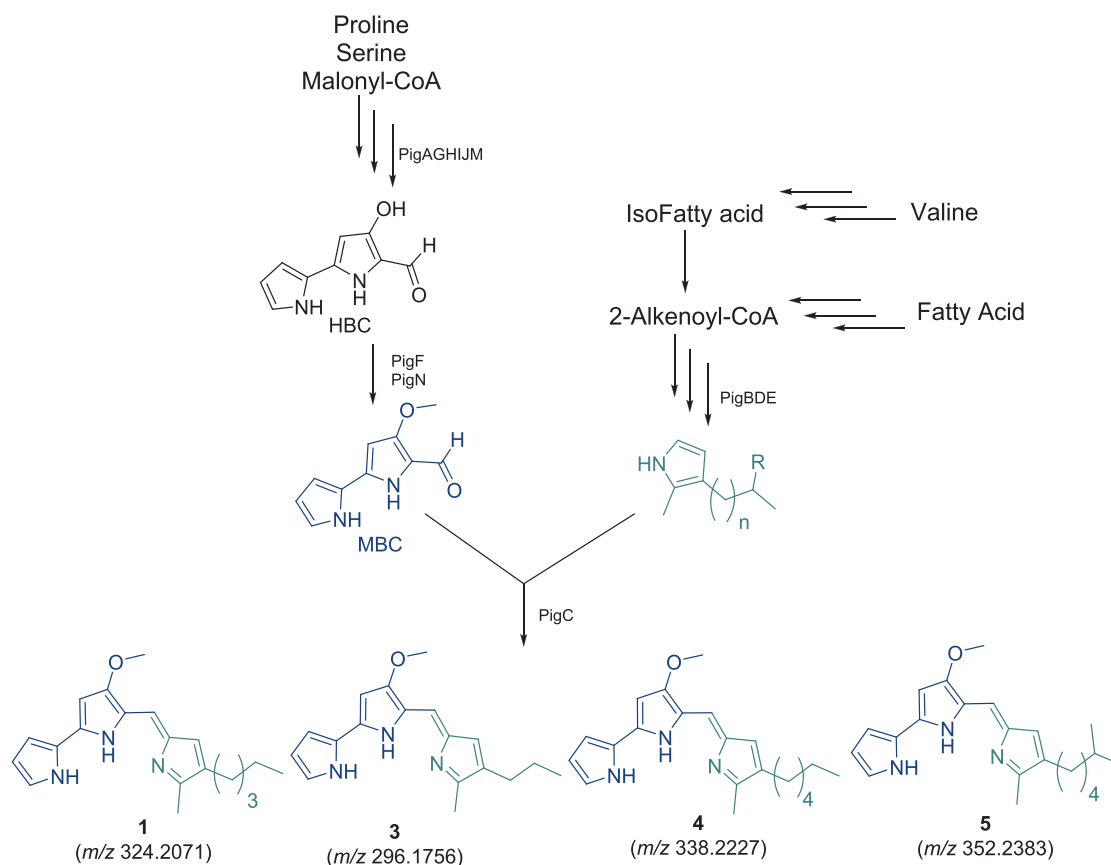


Figure 3. Linear prodigiosins from *Vibrio spartinae* 3.6 ( $m/z$ ,  $[M + H]^+$ ) and their biosynthetic origins.

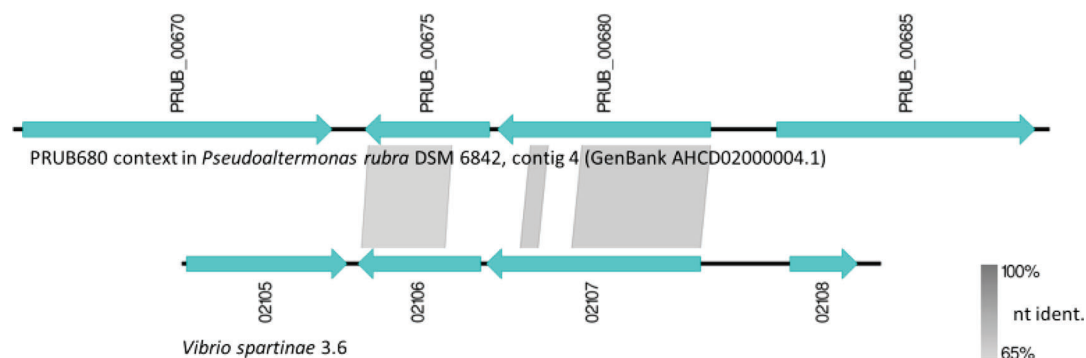


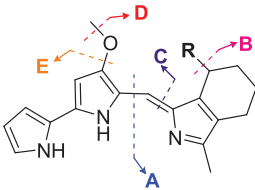
Figure 4. Linear display of PRUB680 and its neighbor PRUB\_00675 found in *P. rubra* DSM 6842, in comparison with their homologues in *V. spartinae* 3.6, Vspart\_02107, and Vspart\_02106.

core, whereas fragments A and D, which differed from each other by +14 amu, were indicative of the presence of homologous side chains at the C-10'' position. Further fragmentation of the daughter fragments A gave the common third-generation fragment  $m/z$  146.0962, due to the loss of the side chain on the cycloprodigiosin core. On the basis of these data, the structures for the compounds correlating to peaks C and E were tentatively assigned as indicated in Table 3, leaving the constitution of the three carbon side chains undetermined, although the iso-propyl chain should be preferred on the basis of biogenetic consideration. This HRMS<sup>n</sup>-comparative genomics approach, highlighted the feature of the fatty acid hydroxylase (Vspart\_02107) to catalyze the regiospecific oxidative cyclization of all the linear prodigiosins to their corresponding six-membered cyclic derivatives, irrespective of

their side chain length. This catalytic capability appears to be a distinctive feature of this enzyme, which is unrelated to previously described proteins involved in the biosynthesis of cyclic prodigiosin-like derivatives.

**Antimicrobial Activities of Pure Molecules.** As reported in the literature, the data on the antimicrobial activity on prodigiosins, mainly cycloprodigiosin and prodigiosin are dated and very limited.<sup>19</sup> In the present study, we evaluated the antimicrobial potential of the new isoheptylprodigiosin (5), together with the major compounds isolated, prodigiosin (1) and cycloprodigiosin (2), against a wide range of human pathogens. Some of the targeted pathogens used in this assay were from the WHO Priority list of pathogens for which new antibiotics are urgently needed,<sup>37</sup> while others are emergent pathogens. A clinical isolate of *L. monocytogenes* was used

Table 3. HRESIMS Analysis of Peaks B, C, and E



	MS <sup>1</sup> ( <i>m/z</i> )	MS <sup>2</sup> fragment ions ( <i>m/z</i> )							MS <sup>3</sup> fragment ion ( <i>m/z</i> ) of fragment A
		R	[M + H] <sup>+</sup>	fragment A	fragment C	fragment D	fragment E	fragment D+B	
peak B cycloprodigiosin 2	CH <sub>3</sub>	322.1914	160.1119	175.0864	307.1676	290.1653	292.1446	146.0962	
		C <sub>20</sub> H <sub>24</sub> N <sub>3</sub> O	C <sub>11</sub> H <sub>14</sub> N	C <sub>10</sub> H <sub>11</sub> N <sub>2</sub> O	C <sub>19</sub> H <sub>21</sub> N <sub>3</sub> O	C <sub>19</sub> H <sub>20</sub> N <sub>3</sub>	C <sub>18</sub> H <sub>18</sub> N <sub>3</sub> O	C <sub>10</sub> H <sub>12</sub> N	
peak C	C <sub>2</sub> H <sub>5</sub>	336.2070	174.1275	175.0863	321.1832	304.1806	292.1442	146.0961	
		C <sub>21</sub> H <sub>26</sub> N <sub>3</sub> O	C <sub>12</sub> H <sub>16</sub> N	C <sub>10</sub> H <sub>11</sub> N <sub>2</sub> O	C <sub>20</sub> H <sub>23</sub> N <sub>3</sub> O	C <sub>20</sub> H <sub>22</sub> N <sub>3</sub>	C <sub>18</sub> H <sub>18</sub> N <sub>3</sub> O	C <sub>10</sub> H <sub>12</sub> N	
peak E	C <sub>3</sub> H <sub>7</sub>	350.2227	188.1431	175.0863	335.1986	318.1962	292.1441	146.0961	
		C <sub>22</sub> H <sub>28</sub> N <sub>3</sub> O	C <sub>13</sub> H <sub>18</sub> N	C <sub>10</sub> H <sub>11</sub> N <sub>2</sub> O	C <sub>21</sub> H <sub>25</sub> N <sub>3</sub> O	C <sub>21</sub> H <sub>24</sub> N <sub>3</sub>	C <sub>18</sub> H <sub>18</sub> N <sub>3</sub> O	C <sub>10</sub> H <sub>12</sub> N	

Table 4. MIC and MIC<sub>50</sub> Values (μg mL<sup>-1</sup>) for Prodigiosin (1), Cycloprodigiosin (2), and Isoheptylprodigiosin (5) against a Panel of Human Pathogenic Bacteria<sup>a</sup>

	antimicrobial activity (μg/mL)							
	prodigiosin (1)		cycloprodigiosin (2)		isoheptylprodigiosin (5)		positive control <sup>b</sup>	
	MIC	MIC <sub>50</sub>	MIC	MIC <sub>50</sub>	MIC	MIC <sub>50</sub>	MIC	
<i>Staphylococcus aureus</i> ATCC 29213	3.3	0.050	4.0	0.060	27	0.50	2.0	
<i>Staphylococcus aureus</i> ATCC 23235	1.3	0.060	3.3	0.080	21	0.50	2.0	
<i>Staphylococcus aureus</i> 6538P	1.7	0.040	3.3	0.050	21	0.20	1.7	
<i>Staphylococcus epidermidis</i> ATCC 35984	2.0	0.33	3.3	0.50	27	2.7	2.0	
<i>Listeria monocytogenes</i> MB677	1.7	0.16	4.0	0.40	21	3.3	0.80	
<i>Stenotrophomonas maltophilia</i> ATCC 13637	1.7	0.66	3.3	2.0	27	3.3	3.3	
<i>Stenotrophomonas maltophilia</i> ATCC 13636	1.7	0.13	3.3	1.0	27	3.3	4.0	
<i>Stenotrophomonas maltophilia</i> ATCC 700475	2.7	0.50	5.3	1.7	27	4.0	4.0	

<sup>a</sup>Each experiment was repeated at least three times ( $n = 3$ ); the mean value is shown in this table. <sup>b</sup>See Table S3 in the Supporting Information for the antibiotics used as positive controls.

during the antibacterial assay; this bacterium is a foodborne pathogen that is the causative agent of listeriosis, one of the most serious and severe foodborne diseases.<sup>38</sup> This pathogen is developing resistance to many antibiotics commercially in use;<sup>39</sup> particularly, the strain used during this assay was isolated from the cerebrospinal fluid of an infected patient. Three strains of *S. maltophilia* were also used, as it is one of the leading drug-resistant nosocomial-associated pathogens.<sup>22</sup> The majority of the clinical isolate strains have developed resistance to multiple agents used to treat Gram-negative bacterial infections.<sup>40,41</sup> The three pigments showed activity toward both Gram-positive and Gram-negative strains, with prodigiosin (1) showing the lowest MIC values (1.3–3.3 μg/mL) and being approximately 2-fold more active than cycloprodigiosin. The MIC and MIC<sub>50</sub> values are reported in Table 4.

The MIC values against *Staphylococcus* species conform with previous presented data.<sup>19,42</sup> The antibacterial activity toward *L. monocytogenes* was compared to ampicillin, which is currently used alone or mixed with gentamicin as the drug of choice for listeriosis treatment,<sup>43–45</sup> and the MIC value of 1 was comparable with the positive control. Moreover, the three prodigiosins were tested on three different *S. maltophilia* strains; also in this case, prodigiosin (1) displayed the best MIC values (1.7–2.7 μg/mL). Among the tested compounds, isoheptylprodigiosin (5) displayed higher MIC values toward all the tested strains.

It is also worth noting the ability of these pigments to inhibit 50% of bacterial growth at sub-MIC concentrations, in particular of Gram-positive pathogens.

Noteworthy is the antimicrobial activity of 1 against *L. monocytogenes* and *S. maltophilia*, particularly as they are the causative agents of difficult to treat infections that urgently require new antibiotic molecules to counteract them.

Herein, we provide a deep elucidation of the structure–function properties of these novel molecules. In particular, the steric hindrance represented by the presence of a branched chain in the isoheptylprodigiosin (5) and of the condensed cycle in the cycloprodigiosin (2) negatively affects their inhibitory capacity.

In conclusion, the whole genomic analysis of the marine bacterial strain *V. spartinae* 3.6, isolated from the sediments of the Rio Formosa lagoon in Portugal, and the metabolic pathway prediction revealed the presence of a prodigiosin BGC. Complete dereplication of the metabolic profile by HRESIMS and NMR analysis led to the identification of five prodigiosins, including the first example of a branched-chain prodigiosin derivative arising from a *pig* gene cluster. The production of the branched-chain molecule was assigned to the peculiar substrate flexibility of the *pigD* homologue in the prodigiosin biosynthetic gene cluster of *V. spartinae* 3.6.

Analogously, the presence of two further homologues of cycloprodigiosin together with a high % of cycloprodigiosin

(more than 50% w/w compared with prodigiosin) was associated with the presence in the *Vibrio* BGCs of a gene encoding for a new member of the alkylglycerol monooxygenase-like enzyme, related to PRUB680 in *P. rubra*. Further investigation of the catalytic properties of this enzyme could expand the biochemical toolbox for the chemoenzymatic transformation of linear precursors of natural and unnatural molecules into their cyclic counterparts via  $\text{sp}^3$  C–H activation, a remarkable process that is often not accessible via conventional synthetic methods.

## EXPERIMENTAL SECTION

**General Experimental Procedures.** UV spectra were recorded with a Varian Cary 1E UV/vis double ray spectrophotometer (Agilent), in MeOH + 0.1% (v/v) trifluoroacetic acid (TFA) at room temperature. 1D and 2D NMR experiments were recorded on Varian Inova 700 (Agilent) and Bruker Avance NEO 400 spectrometers with an RT-DR-BF/1H-5 mm-OZ SmartProbe. Chemical shifts were reported in  $\delta$  (ppm) and were referenced to the residual  $\text{CHCl}_3$  as internal standards ( $\delta_{\text{H}}$  7.26 and  $\delta_{\text{C}}$  77.0).

The LC-HRMS analysis were carried out on an LTQ XL liquid chromatography high-resolution mass spectrometry system (LC-HRMS) (ThermoScientific) equipped with an Accelera 600 pump HPLC. Purification was performed using a Jasco PU-2089 Plus quaternary gradient pump connected to a UV-2075 Plus UV/vis detector equipped with a Waters Rheodine injector for the first purification step and an Acquity UPLC H-CLASS connected to a PDA detector (Waters) for the final purification of the minor components. The 96-well plates were read on a Biotek ELX800, monitoring the absorbance at 600 nm at room temperature.

**Media and Buffers.** All reagents and consumables used in preparation of media were purchased from Conda, Sigma-Aldrich, Merck, or PanReac unless otherwise stated. Media were prepared in grams per liter of ddH<sub>2</sub>O according to the manufacturer's instructions and autoclaved at 121 °C at 15 psi. For the solid media, bacteriological agar was added at 1.7% (w/v).

**Cation-Adjusted Mueller-Hinton Broth (CAMHB).**<sup>46</sup> **Marine Broth (MB):** 19.4 g NaCl, 8.8 g/L MgCl<sub>2</sub>, 5 g/L peptone, 3.24 g/L Na<sub>2</sub>SO<sub>4</sub>, 1.8 g/L CaCl<sub>2</sub>, 1 g/L yeast extract, 0.55 g/L KCl, 0.16 g/L NaHCO<sub>3</sub>, 0.10 g/L Fe(III) citrate, 0.08 g/L KBr, 0.034 g/L SrCl<sub>2</sub>, 0.022 g/L H<sub>3</sub>BO<sub>3</sub>, 0.008 g/L Na<sub>2</sub>HPO<sub>4</sub>, 0.004 g/L sodium silicate, 0.0024 g/L NaF, 0.0016 g/L NH<sub>4</sub>NO<sub>3</sub>

**Tryptone Soy Broth (TSB):** 3 g/L papaic digest of soya, 2.5 g/L D-(+)-glucose, 17 g/L pancreatic digest of casein, 2.5 g/L K<sub>2</sub>HPO<sub>4</sub>, 5 g/L NaCl.

**Marine Broth modified (MB mod):** MB + 10 g/L peptone + 0.3 g/L K<sub>2</sub>HPO<sub>4</sub>.

**Luria–Bertani (LB):** 10 g/L tryptone, 5 g/L yeast extract, 10 g/L NaCl.

**Nutrient broth (NB):** 15 g/L peptone, 6 g/L NaCl, 3 g/L yeast extract.

**Bacterial Strains Isolation.** The bacterial strains were isolated from four sediment sample sites, and six replicates were collected from each site of the Ria Formosa lagoon (Faro, Portugal) and stored at –80 °C until analysis; location coordinates and environmental features are described in Table S1. The rationale for sediment collection was to obtain samples from different environmental conditions and at different depths. For the isolation of bacteria, one gram of each sediment was gently mixed with 3 mL of sterilized water, and the supernatant was serially diluted ( $10^{-1}$  to  $10^{-3}$ ) in sterilized water. A 100  $\mu\text{L}$  amount of each dilution was plated onto MB and TSB agar plates. After 20 days of incubation at 20 °C, 59 morphologically different CFUs were selected and inoculated into MB and TSB liquid media.

**Screening for Antimicrobial Activity.** A single CFU of each of the 59 isolates was inoculated into two 96-well plates, the first filled with 200  $\mu\text{L}$  of MB and the second with TSB, and incubated for 2 days at 20 °C under constant agitation at 120 rpm. Then, the plates

were replicated using a pin replicator into five deep-well plates and filled with 1.6 mL per well of five different media: MB, MB mod, TSB, NB, and LB. Finally, the deep wells were incubated at 20 °C for 5 days, under gentle agitation at 120 rpm. After 5 days, each deep well was replicated onto LB agar plates inoculated with a target pathogenic strain at a concentration of 0.04 OD<sub>600</sub>/mL. *Pseudomonas aeruginosa* O1,<sup>47</sup> *Escherichia coli* ATCC 25922,<sup>48</sup> *Staphylococcus aureus* ATCC 6538P,<sup>49</sup> and *Acinetobacter baumannii* 13<sup>50</sup> were used for these growth inhibition assays.

For the assessment of antimicrobial activity, the plates were inoculated at 20 °C for 24 h to allow the growth of the 59 bacteria. Subsequently, the plates were moved to 37 °C for 24 h to allow the growth of the pathogens, and finally, the active Ria Formosa strains were revealed by the formation of an inhibition halo.

**De Novo Whole Genome Sequence of *Vibrio spartinae* 3.6.** DNA was isolated using Qiagen Genomic-tip 100/G according to the instructions of the manufacturer. A SMRTbell template library was prepared according to the instructions from PacificBiosciences, following the Procedure & Checklist – Greater Than 10 kb Template Preparation. Briefly, for preparation of the 15 kb libraries, 8  $\mu\text{g}$  of genomic DNA from strain 3.6 was applied unshredded. DNA was end-repaired and ligated overnight to hairpin adapters applying components from the DNA/polymerase binding kit P6 from Pacific Biosciences. Reactions were carried out according to the manufacturer's instructions. BluePippin size-selection to greater than 4 kb was performed according to the manufacturer's instructions. Conditions for annealing of the sequencing primers and binding of polymerase to a purified SMRTbell template were assessed with the calculator in RS Remote, PacificBiosciences. One SMRT cell was sequenced per strain on the PacBio RSII taking one 240 min movie. Libraries for sequencing on the Illumina platform were prepared applying the Nextera XT DNA library preparation kit with modifications.<sup>51</sup> Samples were sequenced on NextSeq 500. Genome assembly was performed by applying the RS\_HGAP\_Assembly.3 protocol included in SMRT Portal version 2.3.0 applying a target genome size of 10 Mbp. Error correction was performed by mapping the Illumina short reads onto finished genomes using the Burrows–Wheeler Aligner bwa 0.6.2 in paired-end (sample) mode using default settings,<sup>52</sup> with subsequent variant and consensus calling using VarScan 2.3.6.<sup>53</sup> Automated genome annotation was carried out using Prokka.<sup>54</sup> The genome has been deposited at NCBI GenBank under accession nos. CP046269 and CP046268.

**Species Delineation of *Vibrio spartinae* 3.6 by In Silico Type Strain Genome Server.** The genome sequence data were uploaded to the TYGS, a free bioinformatics platform available at <https://tygs.dsmz.de>, for whole genome-based taxonomic analysis.<sup>55</sup> The results were provided by the TYGS on Oct 2, 2019.

**Primary Metabolism Analysis by KEGG BlastKoala.** The amino acid sequences derived from the nucleotide sequences of the *V. spartinae* 3.6 genome were analyzed by KEGG BlastKoala by selecting “Taxonomy group: Prokaryotes, Bacteria” and the KEGG database searched: “species\_prokaryotes.pep” and other default parameters.

KOALA (KEGG orthology and links annotation) is KEGG's internal annotation tool for K number assignment of KEGG GENES using SSEARCH computation. BlastKOALA assigns K numbers to the user's sequence data by BLAST searches against a nonredundant set of KEGG GENES.<sup>25</sup>

**Strain Cultivation and Metabolite Extraction.** A single CFU of *V. spartinae* 3.6 was used to inoculate 3 mL of liquid MB mod in a sterile bacteriological tube. After 48 h of incubation at 20 °C at 180 rpm, the preinoculum was used to inoculate 200 mL of the same media, at an initial optical density of 0.01 at 600 nm. The flask was incubated for 3 days at 20 °C under constant agitation of 180 rpm. Metabolites were extracted with acetone and EtOAc from the biomass and exhausted broth, respectively; then they were mixed together and evaporated and the obtained extract was dissolved at 1 mg/mL of LC-MS grade MeOH. Finally, 4  $\mu\text{L}$  of extract was injected to carry out the chemical profiling. LC-HRMS dereplication utilized the LC-HRMS instrumentation equipped with an Acquity UPLC BEH C18 1.7  $\mu\text{m}$  column (Waters). The mobile phase A was composed of 100% LC-

MS mass grade H<sub>2</sub>O, and the mobile phase B was composed of 100% MeCN; both phases were added with 0.1% of LC-MS grade formic acid.

**Isolation and Purification of Compounds.** Large-scale fermentation was obtained by inoculating 1.8 L of MB mod. Pigments were extracted with the same methodology described above, and in addition to that, the extract was subjected to a first hexane/MeOH liquid–liquid partitioning (3 × 100 mL), followed by CHCl<sub>3</sub>/H<sub>2</sub>O extraction (3 × 100 mL). Finally, the organic layer was dried over anhydrous sodium sulfate, concentrated under reduced pressure, and lyophilized to give about 300 g of dark extract. The extract was subjected to a first HPLC fractionation on a Phenomenex Luna column (5 μm, 10 mm i.d. × 250 mm) using a gradient program (flow rate 0.3 mL/min; 50 μL injection volume). The mobile phase consisted of 0.1% TFA in H<sub>2</sub>O (buffer A) and 0.1% TFA in MeCN (buffer B), following this gradient program: the initial solvent condition was 45% solvent B for 5 min; the gradient was then gradually increased from 45% solvent B to 85% solvent B over 25 min. Subsequently, solvent B was increased to 100% and was kept at 100% of B for 10 min before the re-equilibration step. The semipreparative fractionation gave 14.5 mg of pure cycloprodiginosin (2) and 26.6 mg of pure prodiginosin (1). The three enriched fractions were subjected to further UPLC purification on a Phenomenex Luna 5 μm PFP column (5 μm, 4.6 mm i.d. × 250 mm), with an optimized elution profile using the same solvents A and B as the mobile phases, and resulted in 2.5 mg of 5'-methyl-4'-propyl prodiginine (3), 0.7 mg of 11'-methyl-4''hexyl prodiginine (4), and 3 mg of isoheptylprodiginosin (5).

**Isoheptylprodiginosin (5):** dark pink, amorphous solid; UV (MeOH, 0.1% TFA) λ<sub>max</sub> (log ε) 537 (4.3), 512 (4.0), 385 (3.1), 371 (3.1), 296 (3.3); <sup>1</sup>H NMR (CDCl<sub>3</sub>, 400 MHz) and <sup>13</sup>C NMR (CDCl<sub>3</sub>, 125 MHz) Table 2; HRESIMS *m/z* 352.2383 [M + H]<sup>+</sup> (calcd for C<sub>22</sub>H<sub>30</sub>ON<sub>3</sub>, 352.2383).

**Minimal Inhibitory Concentration (MIC) Assessment.** The antimicrobial potential of the pure molecules was assessed by the determination of the MIC by the microdilution method and compared with appropriate antibiotics, as described by the Clinical and Laboratory Standard Institute.<sup>46</sup> The tests were performed in CAMHB. DMSO at an initial concentration of 2% (v/v) was used as negative control, to establish the effect on the cell growth of the solvent used to solubilize the compounds. Each compound was dissolved in DMSO and was 2-fold serially diluted from 32 to 0.015 μg/mL in a final volume of 100 μL of CAMHB, in a 96-well microtiter plate (Sarstedt). Essentially, each well contained 50 μL of test compound solution at twice the desired final concentration and was inoculated with 50 μL of bacterial seed culture grown overnight at 37 °C, yielding a final inoculum of 4 × 10<sup>5</sup> CFU/mL in a 100 μL final volume of each well. Finally, each plate was incubated for 20 h at 37 °C. The MIC<sub>50</sub> has been calculated as the minimum concentration that inhibits 50% of cell population growth. The pathogens used in the screening are listed below: *S. aureus* ATCC 29213,<sup>56</sup> *S. aureus* ATCC 23235,<sup>57</sup> *S. aureus* ATCC 6538P,<sup>49</sup> *S. epidermidis* ATCC 35984,<sup>58</sup> *L. monocytogenes* MB677,<sup>59</sup> *S. maltophilia* ATCC 13637,<sup>60</sup> *S. maltophilia* ATCC 13636,<sup>61</sup> and *S. maltophilia* ATCC 700475.<sup>62</sup>

## ■ ASSOCIATED CONTENT

### Supporting Information

The Supporting Information is available free of charge at <https://pubs.acs.org/doi/10.1021/acs.jnatprod.9b01159>.

Additional information (PDF)

## ■ AUTHOR INFORMATION

### Corresponding Authors

**Donatella de Pascale** – Institute of Biochemistry and Cellular Biology, National Research Council (IBBC–CNR), I-80131 Naples, Italy; Stazione Zoologica Anton Dohrn (SZN), I-80121 Naples, Italy; [orcid.org/0000-0002-6732-0901](https://orcid.org/0000-0002-6732-0901);

Phone: +39-081-6132314; Email: [donatella.depascale@szn.cnr.it](mailto:donatella.depascale@szn.cnr.it), [d.depascale@ibp.cnr.it](mailto:d.depascale@ibp.cnr.it)

**Maria Valeria D'Auria** – Department of Pharmacy, University of Naples "Federico II" (UNINA), I-80131 Naples, Italy; Phone: +39-081-678527; Email: [madauria@unina.it](mailto:madauria@unina.it)

### Authors

**Giovanni Andrea Vitale** – Institute of Biochemistry and Cellular Biology, National Research Council (IBBC–CNR), I-80131 Naples, Italy

**Martina Sciarretta** – Department of Pharmacy, University of Naples "Federico II" (UNINA), I-80131 Naples, Italy

**Fortunato Palma Esposito** – Institute of Biochemistry and Cellular Biology, National Research Council (IBBC–CNR), I-80131 Naples, Italy; Stazione Zoologica Anton Dohrn (SZN), I-80121 Naples, Italy

**Grant Garren January** – Institute of Biochemistry and Cellular Biology, National Research Council (IBBC–CNR), I-80131 Naples, Italy

**Marianna Giaccio** – Institute of Biochemistry and Cellular Biology, National Research Council (IBBC–CNR), I-80131 Naples, Italy

**Boyke Bunk** – Leibniz Institute DSMZ-German Collection of Microorganisms and Cell Cultures GmbH, 38124 Braunschweig, German

**Cathrin Spröer** – Leibniz Institute DSMZ-German Collection of Microorganisms and Cell Cultures GmbH, 38124 Braunschweig, German

**Felizitas Bajerski** – Leibniz Institute DSMZ-German Collection of Microorganisms and Cell Cultures GmbH, 38124 Braunschweig, German

**Deborah Power** – Centro de Ciências do Mar (CCMAR), Universidade do Algarve Campus de Gambelas, 8005-139 Faro, Portugal

**Carmen Festa** – Department of Pharmacy, University of Naples "Federico II" (UNINA), I-80131 Naples, Italy; [orcid.org/0000-0001-8879-4332](https://orcid.org/0000-0001-8879-4332)

**Maria Chiara Monti** – Department of Pharmacy, University of Salerno (UNISA), I-84084 Fisciano, SA, Italy; [orcid.org/0000-0002-1337-2909](https://orcid.org/0000-0002-1337-2909)

Complete contact information is available at: <https://pubs.acs.org/doi/10.1021/acs.jnatprod.9b01159>

### Notes

The authors declare no competing financial interest.

## ■ ACKNOWLEDGMENTS

The authors thank the H2020-MSCA-RISE Ocean Medicines, GA 690944, and the H2020-MSCA-ITN-ETN MarPipe, GA 721421, for partial support. This work was partially supported by Ministero dell'Università e della Ricerca (MIUR) PRIN 2017 (2017A95NCJ) Stolen molecules "Stealing natural products from the depot and reselling them as new drug candidates", by the FCT–Foundation for Science and Technology through the project UID/Multi/04326/2019, and by the operational programs CRESCE Algarve 2020 and COMPETE 2020 through project EMBRC.PT ALG-01-0145-FEDER-022121. The authors thank S. Severitt and C. Berg for excellent technical assistance for genome sequencing. Finally, the authors also acknowledge funding for transnational access through the European Union's Horizon 2020 research and innovation program under grant agreement no. 730984, ASSEMBLE Plus project for some experimental activities.

## REFERENCES

- (1) Yip, C. H.; Yarkoni, O.; Ajioka, J.; Wan, K. L.; Nathan, S. *Appl. Microbiol. Biotechnol.* **2019**, *103*, 1667–1680.
- (2) Williamson, N. R.; Fineran, P. C.; Leeper, F. J.; Salmond, G. P. *Nat. Rev. Microbiol.* **2006**, *4*, 887–899.
- (3) Elahian, F.; Moghimi, B.; Dinmohammadi, F.; Ghamghami, M.; Hamidi, M.; Mirzaei, S. A. *DNA Cell Biol.* **2013**, *32*, 90–97.
- (4) Li, D.; Liu, J.; Wang, X.; Kong, D.; Du, W.; Li, H.; Hse, C. Y.; Shupe, T.; Zhou, D.; Zhao, K. *Int. J. Mol. Sci.* **2018**, *19*, 3465–3486.
- (5) Perez-Tomas, R.; Montaner, B.; Llagostera, E.; Soto-Cerrato, V. *Biochem. Pharmacol.* **2003**, *66*, 1447–1452.
- (6) Suryawanshi, R. K.; Patil, C. D.; Borase, H. P.; Narkhede, C. P.; Stevenson, A.; Hallsworth, J. E.; Patil, S. V. *Int. J. Cosmet. Sci.* **2015**, *37*, 98–107.
- (7) Daïri, K.; Yao, Y.; Faley, M.; Tripathy, S.; Rioux, E.; Billot, X.; Rabouin, D.; Gonzalez, G.; Lavallée, J.-F.; Attardo, G. *Org. Process Res. Dev.* **2007**, *11*, 1051–1054.
- (8) Smoot, R. L.; Blechacz, B. R.; Werneburg, N. W.; Bronk, S. F.; Sinicrope, F. A.; Sirica, A. E.; Gores, G. J. *Cancer Res.* **2010**, *70*, 1960–1969.
- (9) Bennett, J. W.; Bentley, R. *Adv. Appl. Microbiol.* **2000**, *47*, 1–32.
- (10) Furstner, A. *Angew. Chem., Int. Ed.* **2003**, *42*, 3582–3603.
- (11) Khanafari, A.; Assadi, M. M.; Fakhr, F. A. *Online J. Biol. Sci.* **2006**, *6*, 1–13.
- (12) Darshan, N.; Manonmani, H. K. *J. Food Sci. Technol.* **2015**, *52*, 5393–5407.
- (13) Lee, J. S.; Kim, Y. S.; Park, S.; Kim, J.; Kang, S. J.; Lee, M. H.; Ryu, S.; Choi, J. M.; Oh, T. K.; Yoon, J. H. *Appl. Environ. Microbiol.* **2011**, *77*, 4967–4973.
- (14) Kim, D.; Kim, J. F.; Yim, J. H.; Kwon, S. K.; Lee, C. H.; Lee, H. K. *J. Microbiol. Biotechnol.* **2008**, *18*, 1621–1629.
- (15) Alihosseini, F.; Lango, J.; Ju, K.-S.; Hammock, B. D.; Sun, G. *Biotechnol. Prog.* **2009**, *26*, 352–360.
- (16) de Rond, T.; Stow, P.; Eigl, I.; Johnson, R. E.; Chan, L. J. G.; Goyal, G.; Baidoo, E. E. K.; Hillson, N. J.; Petzold, C. J.; Sarpong, R.; Keasling, J. D. *Nat. Chem. Biol.* **2017**, *13*, 1155–1157.
- (17) Mo, S.; Sydor, P. K.; Corre, C.; Alhamadsheh, M. M.; Stanley, A. E.; Haynes, S. W.; Song, L.; Reynolds, K. A.; Challis, G. L. *Chem. Biol.* **2008**, *15*, 137–148.
- (18) Stankovic, N.; Senerovic, L.; Ilic-Tomic, T.; Vasiljevic, B.; Nikodinovic-Runic, J. *Appl. Microbiol. Biotechnol.* **2014**, *98*, 3841–3858.
- (19) You, Z.; Zhang, S.; Liu, X.; Zhang, J.; Wang, Y.; Peng, Y.; Wu, W. *Appl. Microbiol. Biotechnol.* **2019**, *103*, 2873–2887.
- (20) Lucena, T.; Arahall, D. R.; Ruvira, M. A.; Navarro-Torre, S.; Mesa, J.; Pajuelo, E.; Rodriguez-Llorente, I. D.; Rodrigo-Torres, L.; Pinar, M. J.; Pujalte, M. J. *Int. J. Syst. Evol. Microbiol.* **2017**, *67*, 3506–3512.
- (21) World Health Organization. *Listeriosis*, 2018. Available online: <https://www.who.int/news-room/fact-sheets/detail/listeriosis>.
- (22) Gajdács, M.; Urbán, E. *Diseases (Basel, Switzerland)* **2019**, *7*, 41.
- (23) Dias, J.; Sousa, M. J. *Coast Res.* **2012**, *56*, 1345–1349.
- (24) Meier-Kolthoff, J. P.; Auch, A. F.; Klenk, H.-P.; Göker, M. *BMC Bioinf.* **2013**, *14*, 1–14.
- (25) Kanehisa, M.; Sato, Y.; Morishima, K. *J. Mol. Biol.* **2016**, *428*, 726–731.
- (26) Feher, D.; Barlow, R. S.; Lorenzo, P. S.; Hemscheidt, T. K. *J. Nat. Prod.* **2008**, *71*, 1970–1972.
- (27) Johnson, R.; de Rond, T.; Lindsay, V.; Keasling, J.; Sarpong, R. *Org. Lett.* **2015**, *17*, 3474–3477.
- (28) Wang, Y.; Nakajima, A.; Hosokawa, K.; Soliev, A. B.; Osaka, I.; Arakawa, R.; Enomoto, K. *Biosci., Biotechnol., Biochem.* **2012**, *76*, 1229–1232.
- (29) Kimata, S.; Matsuda, T.; Suizu, Y.; Hayakawa, Y. *J. Antibiot.* **2018**, *71*, 393–396.
- (30) Kawasaki, T.; Sakurai, F.; Hayakawa, Y. *J. Nat. Prod.* **2008**, *71*, 1265–1267.
- (31) Mo, S.; Kim, B. S.; Reynolds, K. A. *Chem. Biol.* **2005**, *12*, 191–200.
- (32) Hu, D. X.; Withall, D. M.; Challis, G. L.; Thomson, R. J. *Chem. Rev.* **2016**, *116*, 7818–7853.
- (33) Sydor, P. K.; Barry, S. M.; Odulate, O. M.; Barona-Gomez, F.; Haynes, S. W.; Corre, C.; Song, L.; Challis, G. L. *Nat. Chem.* **2011**, *3*, 388–392.
- (34) Withall, D. M.; Haynes, S. W.; Challis, G. L. *J. Am. Chem. Soc.* **2015**, *137*, 7889–7897.
- (35) Bai, Y.; McCoy, J. G.; Levin, E. J.; Sobrado, P.; Rajashankar, K. R.; Fox, B. G.; Zhou, M. *Nature* **2015**, *524*, 252–256.
- (36) Shanklin, J.; Guy, J. E.; Mishra, G.; Lindqvist, Y. *J. Biol. Chem.* **2009**, *284*, 18559–18563.
- (37) World Health Organization. *WHO publishes list of bacteria for which new antibiotics are urgently needed*, 2017. Available online: <https://www.who.int/news-room/detail/27-02-2017-who-publishes-list-of-bacteria-for-which-new-antibiotics-are-urgently-needed>.
- (38) European Food Safety Authority and European Centre for Disease Prevention and Control (EFSA and ECDC). *EFSA J.* **2018**, *19*, e05500.
- (39) Olaimat, A. *Compr. Rev. Food Sci. Food Saf.* **2018**, *17*, 1277–1292.
- (40) Khardori, N.; Reuben, A.; Rosenbaum, B.; Rolston, K.; Bodey, G. P. *Antimicrob. Agents Chemother.* **1990**, *34*, 1609–1610.
- (41) Neu, H. C.; Saha, G.; Chin, N. X. *Diagn. Microbiol. Infect. Dis.* **1989**, *12*, 283–285.
- (42) Herraiz, R.; Mur, A.; Merlos, A.; Vinas, M.; Vinuesa, T. *J. Venomous Anim. Toxins Incl. Trop. Dis.* **2019**, *25*, e20190001.
- (43) Temple, M. E.; Nahata, M. C. *Ann. Pharmacother.* **2000**, *34*, 656–661.
- (44) Allerberger, F.; Wagner, M. *Clin. Microbiol. Infect.* **2010**, *16*, 16–23.
- (45) Davis, J. A.; Jackson, C. R. *Microb. Drug Resist.* **2009**, *15*, 27–32.
- (46) CLSI. *Methods for Dilution Antimicrobial Susceptibility Tests for Bacteria That Grow Aerobically: Approved Standard*, 10th ed.; Clinical and Laboratory Standards Institute: Wayne, PA, 2015; Vol. 35.
- (47) Stover, C. K.; Pham, X. Q.; Erwin, A. L.; Mizoguchi, S. D.; Warrenner, P.; Hickey, M. J.; Brinkman, F. S.; Hufnagle, W. O.; Kowalik, D. J.; Lagrou, M.; Garber, R. L.; Goltry, L.; Tolentino, E.; Westbrook-Wadman, S.; Yuan, Y.; Brody, L. L.; Coulter, S. N.; Folger, K. R.; Kas, A.; Larbig, K.; Lim, R.; Smith, K.; Spencer, D.; Wong, G. K.; Wu, Z.; Paulsen, I. T.; Reizer, J.; Saier, M. H.; Hancock, R. E.; Lory, S.; Olson, M. V. *Nature* **2000**, *406*, 959–964.
- (48) Sauer, A.; Moraru, C. I. *J. Food Prot.* **2009**, *72*, 937–944.
- (49) Connolly, P.; Bloomfield, S. F.; Denyer, S. P. *J. Appl. Bacteriol.* **1994**, *76*, 68–74.
- (50) Corvec, S.; Poirel, L.; Naas, T.; Drugeon, H.; Nordmann, P. *Antimicrob. Agents Chemother.* **2007**, *51*, 1530–1533.
- (51) Baym, M.; Kryazhimskiy, S.; Lieberman, T. D.; Chung, H.; Desai, M. M.; Kishony, R. *PLoS One* **2015**, *10*, 1–15.
- (52) Li, H.; Durbin, R. *Bioinformatics* **2009**, *25*, 1754–1760.
- (53) Koboldt, D. C.; Zhang, Q.; Larson, D. E.; Shen, D.; McLellan, M. D.; Lin, L.; Miller, C. A.; Mardis, E. R.; Ding, L.; Wilson, R. K. *Genome Res.* **2012**, *22*, 568–576.
- (54) Seemann, T. *Bioinformatics* **2014**, *30*, 2068–2069.
- (55) Meier-Kolthoff, J. P.; Göker, M. *Nat. Commun.* **2019**, *10*, 2182.
- (56) Azizkhani, M.; Misaghi, A.; Akhondzadeh Basti, A.; Gandomi, H.; Hosseini, H. *Int. J. Food Microbiol.* **2013**, *163*, 159–165.
- (57) Lima, D.; Torres, A.; Mello, C.; Menezes, R.; Sampaio, T.; Canuto, J.; Silva, J.; Valder, F.; Quinet, Y.; Havt, A.; Monteiro, H.; Nogueira, N.; Martins, A. *J. Appl. Microbiol.* **2014**, *117*, 390–396.
- (58) Christensen, G. D.; Bisno, A. L.; Parisi, J. T.; McLaughlin, B.; Hester, M. G.; Luther, R. W. *Ann. Intern. Med.* **1982**, *96*, 1–10.
- (59) Werbrouck, H.; Vermeulen, A.; Van Coillie, E.; Messens, W.; Herman, L.; Devlieghere, F.; Uyttendaele, M. *Int. J. Food Microbiol.* **2009**, *134*, 140–146.
- (60) Zhang, L.; Li, X. Z.; Poole, K. J. *Antimicrob. Chemother.* **2001**, *48*, 549–552.

(61) Huertas Mendez, N. J.; Vargas Casanova, Y.; Gomez Chimbi, A. K.; Hernandez, E.; Leal Castro, A. L.; Melo Diaz, J. M.; Rivera Monroy, Z. J.; Garcia Castaneda, J. E. *Molecules* **2017**, *22*, 452.

(62) Kaiser, S.; Biehler, K.; Jonas, D. *J. Bacteriol.* **2009**, *191*, 2934–2943.

Article

# Characterization of a New Mixture of Mono-Rhamnolipids Produced by *Pseudomonas gessardii* Isolated from Edmonson Point (Antarctica)

Carmine Buonocore <sup>1</sup>, Pietro Tedesco <sup>1,†</sup>, Giovanni Andrea Vitale <sup>1</sup>, Fortunato Palma Esposito <sup>2</sup>, Rosa Giugliano <sup>3</sup>, Maria Chiara Monti <sup>4</sup>, Maria Valeria D'Auria <sup>5,\*</sup> and Donatella de Pascale <sup>1,2,\*</sup>

<sup>1</sup> Institute of Biochemistry and Cell Biology, National Research Council, 80131 Naples, Italy; carmine.buonocore@ibbc.cnr.it (C.B.); tedesco@insa-toulouse.fr (P.T.); giovanniandrea.vitale@ibbc.cnr.it (G.A.V.)

<sup>2</sup> Department of Marine Biotechnology, Stazione Zoologica Anton Dohrn, Villa Comunale, 80125 Naples, Italy; fpefortunato@gmail.com

<sup>3</sup> Department of Experimental Medicine, University of Campania “Luigi Vanvitelli”, 80138 Naples, Italy; rosa.giugliano@unicampania.it

<sup>4</sup> Department of Pharmacy, University of Salerno, 84084 Salerno, Italy; mcmonti@unisa.it

<sup>5</sup> Department of Pharmacy, University of Naples “Federico II”, 80131 Naples, Italy

\* Correspondence: madauria@unina.it (M.V.D.); donatella.depascale@szn.it (D.d.P.); Tel.: +39-081-5833319 (D.d.P.)

† Current address: TBI-INSA, 135 Avenue de Ranguel, 31400 Toulouse, France.

Received: 20 April 2020; Accepted: 18 May 2020; Published: 20 May 2020



**Abstract:** Rhamnolipids (RLs) are surface-active molecules mainly produced by *Pseudomonas spp.* Antarctica is one of the less explored places on Earth and bioprospecting for novel RL producer strains represents a promising strategy for the discovery of novel structures. In the present study, 34 cultivable bacteria isolated from Edmonson Point Lake, Ross Sea, Antarctica were subjected to preliminary screening for the biosurfactant activity. The positive strains were identified by 16S rRNA gene sequencing and the produced RLs were characterized by liquid chromatography coupled to high resolution mass spectrometry (LC-HRESIMS) and liquid chromatography coupled with tandem spectrometry (LC-MS/MS), resulting in a new mixture of 17 different RL congeners, with six previously undescribed RLs. We explored the influence of the carbon source on the RL composition using 12 different raw materials, such as monosaccharides, polysaccharides and petroleum industry derivatives, reporting for the first time the production of RLs using, as sole carbon source, anthracene and benzene. Moreover, we investigated the antimicrobial potential of the RL mixture, towards a panel of both Gram-positive and Gram-negative pathogens, reporting very interesting results towards *Listeria monocytogenes* with a minimum inhibitory concentration (MIC) value of 3.13 µg/mL. Finally, we report for the first time the antimicrobial activity of RLs towards three strains of the emerging multidrug resistant *Stenotrophomonas maltophilia* with MIC values of 12.5 µg/mL.

**Keywords:** Antarctica; bioprospecting; rhamnolipid; antimicrobials

## 1. Introduction

Among glycolipids, rhamnolipids (RLs) are the best-known and characterized biosurfactants [1], and consist of either one or two rhamnose units linked by a β-glycosidic bond with a 3-(hydroxyalkanoyloxy) alkanic acid (HAA) fatty acid tail ranging between 8 and 16 carbons in length [2]. So far, more than one hundred RL homologues have been discovered, and they differ from

each other mainly in the length of the fatty acid chains and in the degree of unsaturation [3,4]. RLs are involved in motility, enhancing and modulating the swarming movement [5], in the improvement of the uptake of the poorly soluble hydrocarbons [6], in the biofilm formation and structure [7], and antimicrobial activities, such as antibacterial, antifungal, and antialgal [8–11]. In particular, these compounds showed strong activity towards a wide range of bacteria and fungi [12–14].

Cold environments are defined as places permanently exposed to temperatures below 5 °C and account for more than 80% of the Earth's biosphere. The polar regions represent nearby 15% [15] and could represent a huge resource of unexplored natural products, in particular biosurfactants. Indeed, microorganisms living in the cold environment have shown enhanced biosurfactant production to cope with cellular and proteins disruption, due to the ice and water phases cycles, and the carbon sources limitations [16,17]. Antarctica is the coldest and most largely unexplored place on Earth and hosts microbes able of withstanding high selective pressures, such as high UV-radiation, drought, light limitation and extremely low temperatures [18,19]. Therefore, thanks to its selective living conditions, Antarctica harbors many strains with valuable features for biotechnology and therefore, bioprospecting represents a promising strategy for the isolation of strains capable to produce new molecules of interest.

In a previous study, our research group described the isolation and the identification and characterization of two novel RLs produced by a strain isolated from Antarctic shallow water. These RLs showed antimicrobial activity towards *Burkholderia cepacia* complex, a group of opportunist multidrug resistant human pathogens, suggesting a potential role of these molecules in the fight against multi drug resistant bacteria [20].

In this study, the production of RLs by Antarctic bacteria has been investigated. The study involved the isolation of microorganisms, selection of the active strains by three complementary rapid screens for the biosurfactant activity, phylogenetic affiliation of the active strains by 16S rRNA sequencing, cultivation, solvent extraction of metabolites, 16S rRNA sequencing and LC-HRESMS identification of the compounds. Moreover, the influence of the carbon source on the mixture complexity and its antimicrobial ability was also investigated.

## 2. Results and Discussion

### 2.1. Bacterial Isolation and Biosurfactant Activity Screening

Isolation of bacteria from sediments collected from Edmonson Point was performed on marine agar (MA) and TYP agar plates. After 15 days of incubation at 20 °C, 34 morphologically different colonies were selected, 21 from MA plates and 13 from TYP plates.

All the strains were cultured in the respective liquid media. After 5 days of incubation, the culture broths were centrifuged and the supernatants were extracted by ethyl acetate. The obtained crude extracts were screened for biosurfactant activity. Only 3 strains (M15, M38, T28) exhibited positivity to the biosurfactant activity tests, out of 34 bacterial isolates (Figure 1).

The emulsification indexes (E24) [21], the oil spreading in water [22] and the reactions with dyes such as cetyltrimethylammonium bromide (CTAB) [23] were used as complementary assays to detect the production of anionic biosurfactants [24].

The presence of anionic biosurfactants in the extracts of M15, M38 and T28 was confirmed by the arising of a dark blue halo in the CTAB agar plate (Figure 1a). After 48 h at 4 °C, the diameters of the dark blue haloes were detected: M15 (ø 0.88 cm), M38 (ø 0.87 cm), T28 (ø 0.89 cm). SDS 0.1%, positive control showed a 2.16 cm diameter halo. CTAB agar test is specific for anionic biosurfactants, thus, in order to investigate the presence of other biosurfactants in the crude extracts, the oil spreading test was performed. This assay can reveal the presence of biosurfactants through the development of a clear halo in the oil-water surface. Again, the best results were obtained by M15 (ø 2.6 cm) (Figure 1b), while M38 and T28 gave (ø 1.8 cm) and (ø 2.4 cm), respectively. The assessment of E24 (55%, 40%, 50% and 50%, respectively, Figure 1c) using Tween 20<sup>®</sup> as a positive control indicated a remarkable emulsifying power towards n-Hexane.

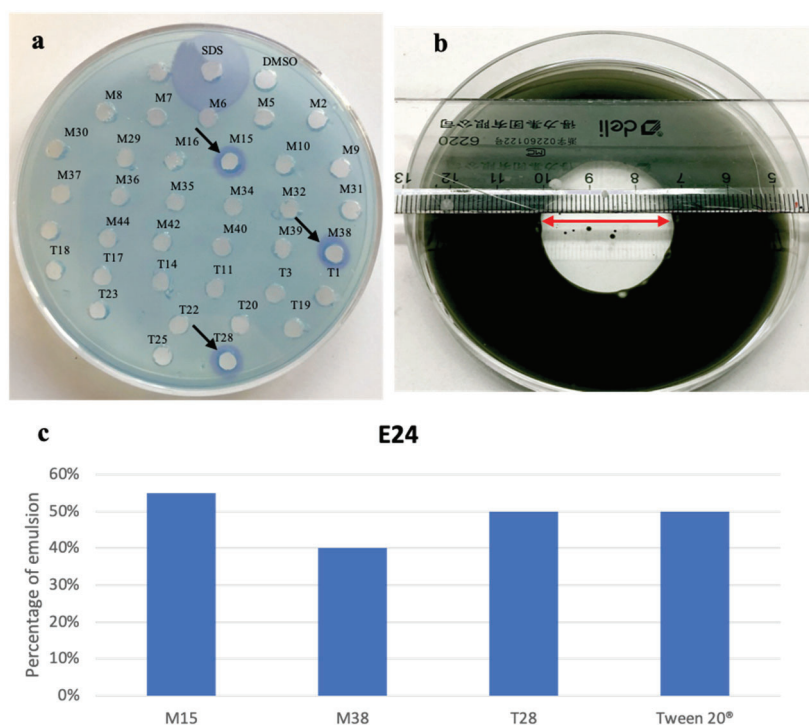


**Figure 1.** (a) Biosurfactants activity on a cetyltrimethylammonium bromide (CTAB) agar plate, the blue halos indicate the positivity to the test, the arrows show the positive extracts; (b) oil spreading test, the red arrows indicate the diameter of the halo; (c) the graph shows the E24 values of the tested supernatants and Tween 20®.

## 2.2. Bacterial Identification

To identify M15, M38 and T28, 16S rRNA amplicons were sequenced and investigated through EzBioCloud [25]. The results were utilized to build a phylogenetic tree with a set of related species (Figure 2). The output of both EzBioCloud and the phylogenetic tree showed that the investigated strains were closely related, if not conspecific, to *P. gessardii* DSM 17152 [26], with values of similarity and variation ratio, respectively, of 99.43% and 8/1412 bp for M15, 99.78% and 3/1344 bp for M38, and 99.93% and 1/1351 bp for T28. *P. gessardii* belongs to the *P. fluorescence* group that was already reported to produce rhamnolipids [27]; moreover, a strain closely related to *P. gessardii* and able to produce RLs was recently isolated in Antarctica [28].

Therefore, giving the close phylogenetic relationship between the three selected strains, only the most active M15 was selected for further investigation.

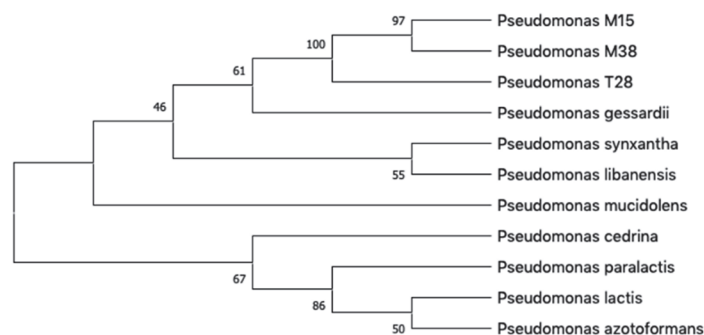


**Figure 2.** Phylogenetic tree generated with MEGAX based on 16S rRNA gene sequences of M15, M38 and T28 strains and related species. Next to the branches are shown the percentage of replicate trees in which the associated taxa clustered together in the bootstrap test.

### 2.3. Chemical Characterization

The crude ethyl acetate extract was subjected to first fractionation by solid-phase extraction (SPE) with C-18 cartridges as described in Materials and Methods. In order to confirm the activity, the obtained fractions were subjected once again to CTAB agar and oil-spreading assay. Fractions eluted at 80% and 100% methanol (MeOH) showed positivity to both assays. No activity was shown by the fraction eluted at 60% MeOH.

The 80%- and 100%-MeOH fractions, both positive to the biosurfactant activity tests, were subjected to LC-HRESMS dereplication in both positive and negative modes. The total ion chromatograms recorded in negative mode (Figure 3) of both fractions displayed a similar pattern, indicating a complex mono-rhamnolipid mixture. As extensively reported in the literature [29–31], the analysis of the negative pseudo-molecular ion  $[M - H]^-$  obtained by LC-HRESMS gave information on the molecular formula. Under the experimental conditions used for the analysis, the primary ion underwent spontaneous in-source fragmentation, giving rise to the key fragment ion arising from the cleavage of the ester linkage between the two  $\beta$ -hydroxy fatty acid units, allowing the discrimination between congeners with non-symmetric fatty acid units. For instance, the molecular formula  $C_{24}H_{44}O_9$  for the peak at 14.22 min (Figure 3a) corresponds to a Rha-C<sub>8</sub>-C<sub>10</sub> or Rha-C<sub>10</sub>-C<sub>8</sub> structure. The key fragment at  $m/z$  305.1290, observed in the mass spectra (S1. Supplementary Materials) corresponding to Rha-C<sub>8</sub>, allowed us to assign the Rha-C<sub>8</sub>-C<sub>10</sub> structure.

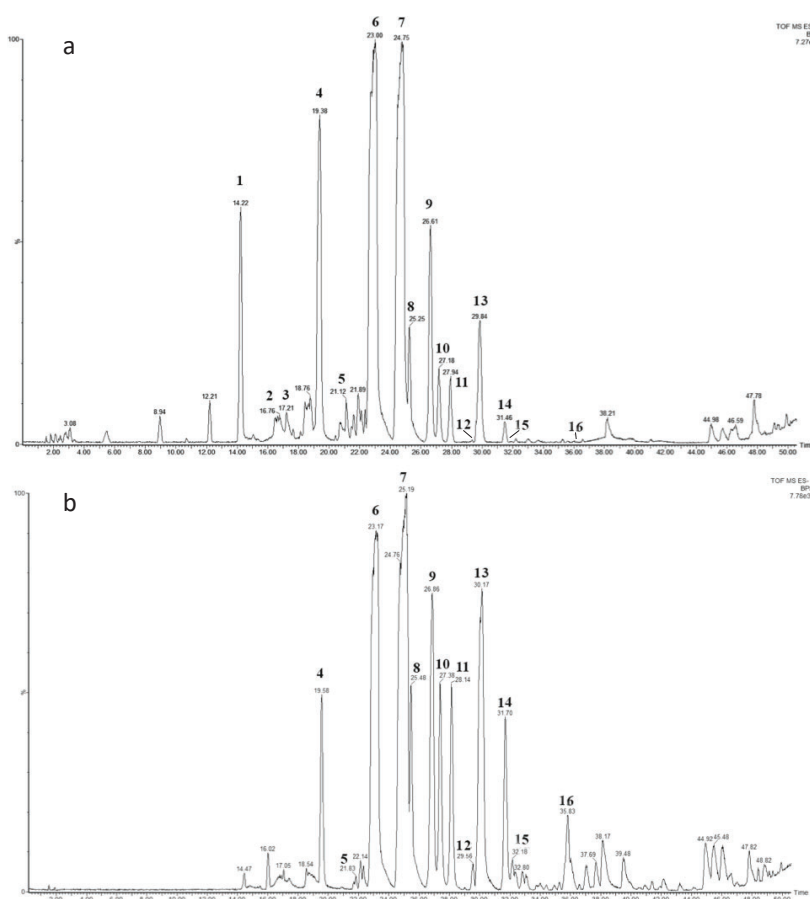


**Figure 3.** Total ion chromatogram of: (a) M15 SPE 80% and (b) M15 SPE 100% fractions. The rhamnolipids (RLs) peaks are numerated and shown in Table 1.

Mass spectra dereplication highlighted the presence of a total of 16 different mono-RLs, about half of them displayed the presence of at least one unsaturation in one of the fatty acid (FA) chains (Table 1).

Compounds 3, 8, 12, 14 and 15 are described for the first time in this work, while the other are already present in literature [32,33].

The fragmentation of the  $[M - H]^-$  adducts of the five new RLs led to three key ions for each one, Rha-FA1, FA1-FA2 and FA2, which further confirmed the previously hypothesized structure for the compounds 3, 8, 12 and 14 (Figure 4a–d). The compound 15, submitted to MS/MS fragmentation, gave the simultaneous presence of the daughter ions 223, 361 and 421, respectively, due to  $C_{12}$ , Rha- $C_{12}$  and  $C_{12}$ - $C_{14:1}$ , together with the ions derived from the fragmentation of Rha- $C_{14:1}$ - $C_{12}$  (Figure 4e), highlighting the co-occurrence of the two structural isomers, Rha- $C_{14:1}$ - $C_{12}$  and Rha- $C_{12}$ - $C_{14:1}$ .

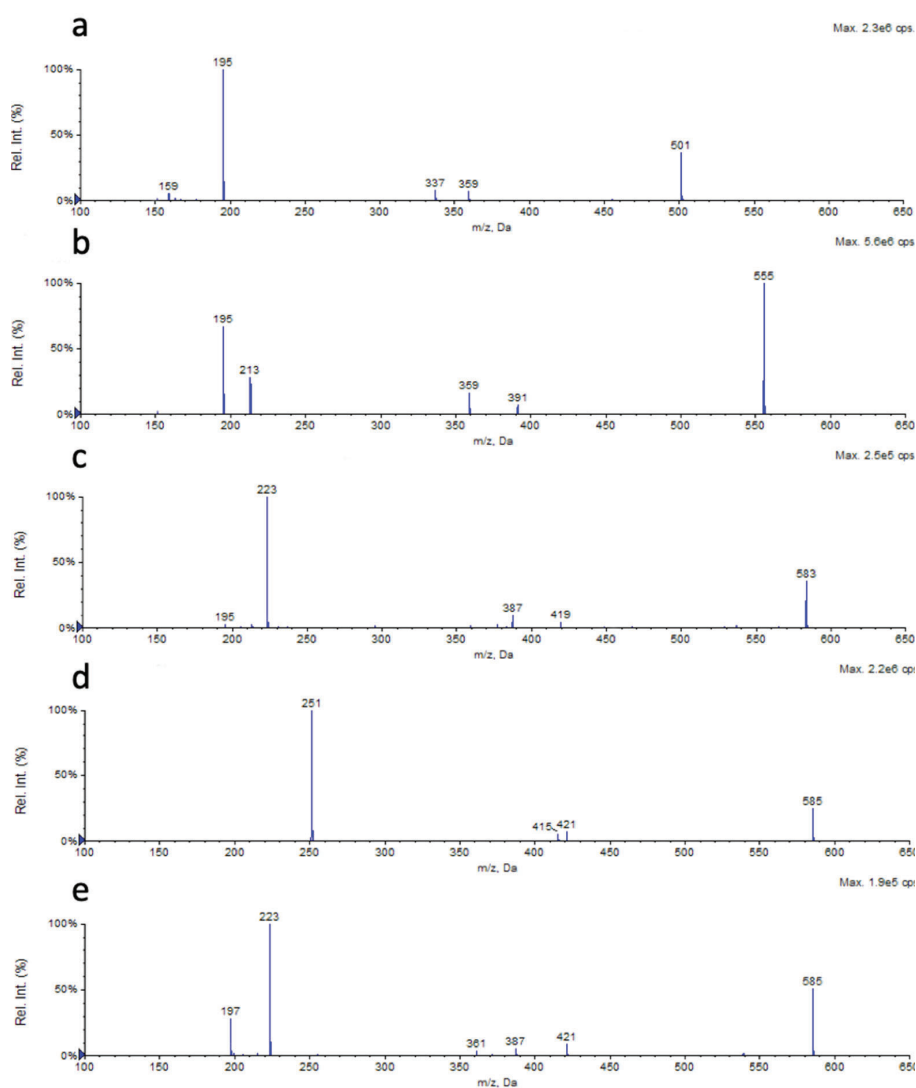


**Figure 4.** The MS/MS spectra of the new RLs (a) Rha- $C_{12:1}$ - $C_8$ , (b) Rha- $C_{12:1}$ - $C_{12:1}$ , (c) Rha- $C_{14:1}$ - $C_{12:1}$ , and (d) Rha- $C_{16:1}$ - $C_{10}$  confirmed their structure predicted on the basis of their in-source fragmentation. (e) The MS/MS spectra of the compound under the peak 15 showed the presence of the two RLs Rha- $C_{14:1}$ - $C_{12}$  and Rha- $C_{12}$ - $C_{14:1}$ .

These molecules are all characterized by the presence of an unsaturation on the FA1 chain, the compounds 8 and 12 also displayed an additional unsaturation on FA2 chain. *P. gessardii* has been reported in the literature for the production of biosurfactants such as RLs [28] and a lipoprotein [34]. In particular, Kristoffersen et al. [28] reported the production of five mono-rhamnolipids with the same formula of compounds 4, 6, 7 and 9 found in this work (Table 1).

**Table 1.** Assignment of the identified RLs present in the LC-MS TICs of M15 80% and 100% fractions (Figure 3) <sup>a</sup>.

No.	Retention Time (min)	Measured [M – H] <sup>–</sup> (m/z)	Δ ppm vs. Theoretical Value	Molecular Formula	Key Fragment (Rha-FA1)	RL	n <sub>1</sub>	n <sub>2</sub>	Structure
1	14.22	475.2779	–26.9	C <sub>24</sub> H <sub>44</sub> O <sub>9</sub>	305.1290	Rha-C <sub>8</sub> -C <sub>10</sub>	1	3	
2	16.76	489.3087	+4.7	C <sub>25</sub> H <sub>46</sub> O <sub>9</sub>	319.1520	Rha-C <sub>9</sub> -C <sub>10</sub>	2	3	
3	17.21	501.2946	–23.5	C <sub>26</sub> H <sub>48</sub> O <sub>9</sub>	359.2195	Rha-C <sub>12:1</sub> -C <sub>8</sub>	5(-2H)	1	
4	19.38	503.3036	–36.6	C <sub>26</sub> H <sub>48</sub> O <sub>9</sub>	333.1660	Rha-C <sub>10</sub> -C <sub>10</sub>	3	3	
5	21.12	517.3278	–12.1	C <sub>27</sub> H <sub>50</sub> O <sub>9</sub>	381.2199	Rha-C <sub>11</sub> -C <sub>10</sub>	4	3	
6	23.00	529.3102	–52.0	C <sub>28</sub> H <sub>50</sub> O <sub>9</sub>	359.1872	Rha-C <sub>12:1</sub> -C <sub>10</sub>	5(-2H)	3	
7	24.75	531.3319	–40.3	C <sub>28</sub> H <sub>52</sub> O <sub>9</sub>	361.2039	Rha-C <sub>12</sub> -C <sub>10</sub>	3	3	
8	25.26	555.3454	–14.2	C <sub>30</sub> H <sub>52</sub> O <sub>9</sub>	359.1942	Rha-C <sub>12:1</sub> -C <sub>12:1</sub>	5(-2H)	5(-2H)	
9	26.63	557.3553	–24.6	C <sub>30</sub> H <sub>54</sub> O <sub>9</sub>	387.2223	Rha-C <sub>14:1</sub> -C <sub>10</sub>	7(-2H)	3	
10	27.17	557.3553	–24.6	C <sub>30</sub> H <sub>54</sub> O <sub>9</sub>	361.2039	Rha-C <sub>12</sub> -C <sub>12:1</sub>	5	5(-2H)	
11	27.94	557.3641	–8.8	C <sub>30</sub> H <sub>54</sub> O <sub>9</sub>	359.1872	Rha-C <sub>12:1</sub> -C <sub>12</sub>	5(-2H)	5	
12	29.52	583.3678	–28.8	C <sub>32</sub> H <sub>56</sub> O <sub>9</sub>	387.2296	Rha-C <sub>14:1</sub> -C <sub>12:1</sub>	7(-2H)	5(-2H)	
13	29.84	559.3688	–28.2	C <sub>30</sub> H <sub>56</sub> O <sub>9</sub>	389.2431	Rha-C <sub>14</sub> -C <sub>10</sub>	7	3	
14	31.46	585.3919	–14.3	C <sub>32</sub> H <sub>58</sub> O <sub>9</sub>	415.2556	Rha-C <sub>16:1</sub> -C <sub>10</sub>	9(-2H)	3	
15	32.20	585.3919	–14.3	C <sub>32</sub> H <sub>58</sub> O <sub>9</sub>	387.2296	Rha-C <sub>14:1</sub> -C <sub>12</sub>	7(-2H)	5	
16	35.85	587.4017	–24.2	C <sub>32</sub> H <sub>60</sub> O <sub>9</sub>	417.2728	Rha-C <sub>12</sub> -C <sub>14:1</sub>	5	7(-2H)	
						Rha-C <sub>16</sub> -C <sub>10</sub>	9	3	

<sup>a</sup> Rha denotes the α-L-rhamnopyranosyl moiety, the designation C<sub>x</sub> means a fatty acid chain with chain length of X, C<sub>x:1</sub> means a fatty acid chain with chain length of X and with one unsaturated bond (–2H).

#### 2.4. Analysis of the Influence of the Carbon Source on the RL Chemical Composition

The preference in the carbon source is strain-dependent and may greatly influence the RLs composition [35–39]. Moreover, carbon source has a great impact also in the industrial production economy of the RLs, as it accounts for the 10–30% of the total costs for recombinant production process [40]. Therefore, the capability of a strain to use using low cost or waste materials such as glycerol and used cooking oil (UCO) represent a great advantage. Glycerol is a byproduct of biodiesel industry and its market cannot accommodate the amount generated [40], UCO is a kitchen-generated waste that causes serious environmental problems. When collected, it is utilized mainly in biodiesel production, but can find utilization as a carbon source in fermentation process [41].

M15 strain was grown in the presence of different carbon sources, in order to explore as them affect the RLs mixture composition. Moreover, the ability to produce RLs from petroleum derivate hydrocarbons, both aromatic and aliphatic, as sole carbon source was also explored in a bioremediation context.

Phosphate-limited peptone-ammonium salt (PPAS) medium was utilized as minimal medium, as modification of PPGAS (phosphate-limited peptone-glucose-ammonium salt) [5], and after the incubation, the cell-free broths were extracted and subjected to LC-MS analysis to investigate the presence of RLs.

Isolate M15 was able to utilize all the tested carbon sources for growth while no growth was detected when cultivated in PPAS not supplemented with a carbon source. However, the composition of the RLs mixture was greatly affected by the different carbon sources.

To evaluate these changes in the composition, base peak chromatograms were manually integrated and the relative abundance of the single RL peak, in the RLs mixture, was calculated for each growth condition (Table 2). TYP crude extract (CE) was used as reference condition, detecting RLs 6 and 7 as the most abundant with more than 20% each, followed by RLs 1, 4, 9, and 13 with a relative abundance of near 10%. RLs 8, 10, and 11 accounted for less than 4%, RLs 14 and 16 for less than 2%, while all the others RLs were less than 1% of the total composition.

Among monosaccharides, glucose and mannose gave better results than rhamnose in term of numbers of congeners production, but the relative abundance of the single RLs was very dissimilar. In fact, in mannose, the RLs 1, 6 and 7 accounted for more than 80% of the entire mixture, while in glucose the same compounds were less than 60%. Out of the three monosaccharides, rhamnose gave the worst results in terms of RL congeners production; in fact, eight RLs were completely missing or drastically reduced, while the presence of compounds 2 and 6 in the mixture were quadrupled and doubled, respectively. The polysaccharides starch and xylan gave very similar results, with a difference represented by compounds 10–13, which are not present in xylan, while in starch were present three times more than TYP CE.

Glycerol showed the presence of all the RLs and together with UCO exhibited the highest relative abundance of the new RLs. In particular, compound 3 in glycerol and UCO was ten and six times more abundant than in TYP CE, respectively. RLs 8, 14 and 15 were doubled in both conditions, while the abundance of RL 2 was more than quadrupled in UCO.

Considering petroleum derived carbon sources, diesel gave an interesting mixture, in which the quadrupled production of RLs 2 and 3 and the lack of 15 and 16 were the most significant results. The relative composition of the benzene was afflicted by the lack or drastic reduction in RLs 5, 10, 11, 13, 14, 15, and 16, while the quadrupled abundance of compound 12 was notable. Among polyaromatic hydrocarbons (PAH), anthracene gave remarkable results, showing the presence of 11 RLs on a total of 16. To the best of our knowledge, benzene and anthracene were reported here for the first time as the sole carbon source in RLs production. Finally, the production of RLs was not detected in pyrene, while on phenanthrene, only RL 6 (Figures S17–S29) was found. Singh and Tiwary reported the use of these two PAHs as the sole carbon source for glycolipids production from *Pseudomonas otitidis*, but the glycolipids class was not specified [42].

**Table 2.** Relative abundance of the different rhamnolipid congeners in mixture detected in each growth condition.

Carbon Source	RL Relative Abundance (%)															
	1	2	3 *	4	5	6	7	8 *	9	10	11	12 *	13	14 *	15 *	16
<b>Monosaccharides</b>																
Glucose	10.4		1.6	15.1		23.4	25.1	3.4	8.5	1.4	2.8	0.2	6.2	0.6	0.2	1.1
Mannose	27.9	0.1	0.4	5.9		29.3	25.1	2.4	5.1	0.6	0.8	0.1	1.5	0.5		0.3
Rhamnose	13.2	0.6	0.2	6.1		42.9	32.4	1.2	2.4	0.6	0.4					
<b>Polysaccharides</b>																
Starch	29.6			9.2		36.4	19.8	0.6	2.6	0.2	0.3	0.9	0.4			
Xylan	18.9			9.7		50.1	18.8	0.9	1.6							
<b>Fatty acids and derivatives</b>																
Glycerol	5.2	0.2	5.3	9.5	0.5	19.1	14.0	8.0	12.5	1.9	5.0	0.3	11.8	4.7	1.0	1.0
UCO	5.9		3.2	13.4		17.4	17.0	10.7	5.4	2.6	6.4	1.3	12.2	3.3	1.0	0.2
<b>Petroleum derivatives</b>																
Benzene	24.1	0.3	0.2	6.4		37.3	25.5	2.0	2.0	0.3	0.6	1.3				
Diesel	22.7	0.6	2.2	10.8	0.5	30.4	22.8	1.9	2.7	0.8	1.1	0.3	2.7	0.5		
PAHs																
Anthracene	4.6			9.0	1.2	28.4	50.2	1.0	2.1	0.3	0.6		2.4	0.2		
Phenanthrene						100.0										
Pyrene																
<b>Miscellaneous</b>																
TYP CE	8.5	0.1	0.5	11.1	0.8	21.7	24.1	4.0	7.4	4.9	4.0	0.3	9.4	1.7	0.5	1.0
TYP 80%	10.4	2.5	2.1	12.5	1.3	16.9	22.2	6.2	7.8	2.0	4.2	0.1	10.7	0.9	0.1	0.1
TYP 100%				6.1	2.6	16.9	21.9	7.9	8.5	10.4	6.1	1.4	11.2	4.4	0.6	2.0
Control																

\* New RLs found in this study.

Glycerol and UCO gave the best results in congeners production. This can be explained through consideration on the availability of the RLs precursors, L-rhamnose and 3-hydroxyalkanoate. Thanks to metabolism flexibility, these two metabolites can be produced from many carbon sources, such as sugars, vegetable oils, glycerol, and hydrocarbons, although with a different metabolic cost for the cells [43]. However, fatty acids can be directly incorporated in the lipidic chains of RLs and this can explain the higher number of congeners when the strains are using UCO as a carbon source. On the other hand, glycerol was already reported as a good soluble carbon source for RL production, since it could act as a close biosynthetic precursor of both lipid and sugar building blocks in RL synthesis [44].

RLs are well-known for their bioremediation potential and they have been proven to help in PAH degradation by reducing their hydrophobicity and enhancing their biodegradation by the microbial community [45,46]. Considering M15 capability of producing RLs from pollutants such as anthracene, benzene and diesel, this strain proves to be a suitable candidate for bioremediation applications.

### 2.5. Antimicrobial Activity

The M15 SPE fractions were evaluated for their antimicrobial activity by liquid inhibition assays towards 17 human pathogen bacteria (Table 3). The fraction eluted at 60% of MeOH did not show activity. On the other hand, fractions eluted at 80% and 100% of MeOH were shown to be active towards the majority of the tested Gram-positive bacteria. This evidence is in accordance with the literature [47,48] and can be explained by the ability of biosurfactants to disrupt membrane structure disturbing interactions with phospholipids and membrane proteins of Gram-positive bacteria [49]. Both TYP 80% and 100% fractions showed very low MIC values towards *B. cereus*, *L. monocytogenes*, *S. aureus* strains and *S. epidermidis* with values in that vary from 6.25 to 25 µg/mL for the former and from 3.13 to 25 µg/mL for the latter. Differently from others Gram-positive bacteria, *S. xylosus* showed no sensitivity in the tested concentrations, while *S. epidermidis* showed low sensitivity, with MIC values of 50 and 100 µg/mL for the 80% and 100% fractions, respectively.

**Table 3.** Antimicrobial activity of M15 MeOH fractions reported as minimum inhibitory concentration (MIC) value.

Strains	Minimum Inhibitory Concentration (µg/mL)			Strains	Minimum Inhibitory Concentration (µg/mL)		
	60%	80%	100%		60%	80%	100%
<b>Gram-Positive</b>				<b>Gram-Negative</b>			
<i>B. cereus</i>	-	6.25	3.13	<i>S. maltophilia</i> 700475	-	12.5	25.0
<i>L. monocytogenes</i>	-	25.0	12.5	<i>S. maltophilia</i> 13637	-	12.5	12.5
<i>S. aureus</i> 29213	-	12.5	25.0	<i>S. maltophilia</i> 13636	-	12.5	25.0
<i>S. aureus</i> 23235	-	12.5	12.5	<i>A. baumannii</i>	-	-	-
<i>S. aureus</i> 6538P	-	25.0	25.0	<i>B. metallica</i>	-	-	-
<i>S. epidermidis</i>	-	50.0	100	<i>E. coli</i>	-	-	-
<i>S. xylosus</i>	-	-	-	<i>K. pneumoniae</i>	-	-	-
				<i>P. aeruginosa</i>	-	-	-
				<i>S. Enteritidis</i>	-	-	-
				<i>S. Typhimurium</i>	-	-	-

Although antimicrobial activity of RLs towards Gram-negative bacteria is not uncommon [20,50], generally these bacteria are resistant to anionic surfactants because their outer membrane is hardly permeable to hydrophobic and amphipathic molecules [48,51,52]. Despite *A. baumannii*, *B. metallica*, *E. coli*, *K. pneumoniae*, *P. aeruginosa*, *S. Enteritidis* and *S. Typhimurium* being resistant to the fractions in the tested concentrations, *S. maltophilia* strains showed high sensitivity to them, with a MIC value of 12.5 µg/mL for the 80% fraction and 25 µg/mL for the 100% towards strains 700475 and 13636, while strain 13637 showed higher sensitivity, with a MIC value of 12.5 µg/mL for both fractions. This is a very promising finding, as *S. maltophilia* possesses high level of intrinsic resistance to many antimicrobials and it is also readily able to acquire multidrug resistance when exposed to different antibiotics [53,54].

To the best of our knowledge, this is the first report of a mixture of mono-RLs displaying activity towards *S. maltophilia*.

All the tested pathogens showed sensitivity only to the fractions containing RLs and, although there are some minority unidentified compounds in the fractions, we can speculate that these molecules could be responsible for the antimicrobial activity.

As the antimicrobial activity towards the different strains of both *S. aureus* and *S. maltophilia* were similar, the antimicrobial activity of glucose, mannose, rhamnose, glycerol, and TYP CE extracts were evaluated towards a restricted panel of pathogens, such as *B. cereus*, *L. monocytogenes*, *S. aureus* 23235, *S. epidermidis*, *S. maltophilia* 13637 (Table 4). As reported, different factors affect the antimicrobial activity of both RLs and RLs mixture, such as the congeners composition, the length of the acyl chains, and the presence of unsaturation [20,28,50]. The relative RL composition of glucose, mannose rhamnose, glycerol, xylan, starch and TYP CE extracts (Table 2) was matched with their MIC values (Table 4), allowing us to link the antimicrobial power to a restricted range of congeners. The variations in both the RLs mixture composition and in antimicrobial activity were compared to the TYP CE that was utilized as a reference. The best antimicrobial activities were obtained by the glycerol and two TYP SPE 80% and 100% fractions extracts, which showed the highest relative abundance in the mixture of RLs 8 and 9, and of RLs from 10 to 16. This evidence was particularly highlighted on glycerol, in which relative abundances of RL 8, RL 9 and RL 14, compared to TYP CE, were doubled, 1.5 times more and nearly tripled, respectively. On the contrary, the abundance of RLs 8, 9 and 14 was drastically reduced in mannose and rhamnose that showed low and absent antimicrobial activity, respectively, while they are nearby absent in starch and xylan that showed no activity. This might suggest that RLs 8, 9 and 14 could be the major RLs responsible for the antimicrobial activity. Moreover, the antimicrobial activity of 9 was already reported in the literature [28], while compound 8 and 14 were reported here for first time along with their bioactivity.

**Table 4.** Antimicrobial activity of different growth conditions crude extracts reported as MIC values.

Strains	Minimum Inhibitory Concentration ( $\mu\text{g/mL}$ )						
	Glucose	Mannose	Rhamnose	Glycerol	TYP	Xylan	Starch
<b>Gram-positive</b>							
<i>B. cereus</i>	6.25	100	-	3.13	7.81	-	-
<i>L. monocytogenes</i>	25.0	-	-	3.13	62.5	-	-
<i>S. aureus</i> 6538P	37.5	100	-	6.25	98.3	-	-
<i>S. epidermidis</i>	-	-	-	3.13	62.5	-	-
<b>Gram-negative</b>							
<i>S. maltophilia</i> 13637	50.0	-	-	3.13	62.5	-	-

### 3. Materials and Methods

#### 3.1. Isolation of Microorganisms

Bacterial strains were isolated from sediments collected in Edmonson Point Lake, Ross Sea, Antarctica, 74° 20' (74.3333°) South, 165° 8' (165.1333°) East. To obtain a cells suspension, 1 g of sediments was mixed with 20 mL of M9 salts solution in a 50mL Falcon sterile tube and gently mixed. The suspension was homogenized using a vortex, serially diluted ( $10^{-1}$ ,  $10^{-2}$  and  $10^{-3}$  in 10 mL of M9) and 100  $\mu\text{L}$  of each dilution was plated on MA and TYP agar and incubated at 20 °C for 15 days. After the incubation period, morphologically different colonies were picked, grown in liquid marine broth (MB) and TYP and stored at  $-80$  °C.

#### 3.2. Media and Buffers

The following media and buffers were used during this study:

**M9 salts** (3 g/L  $\text{KH}_2\text{PO}_4$ , 6 g/L  $\text{Na}_2\text{HPO}_4$ , 5 g/L NaCl, 1 mL 1 M  $\text{MgSO}_4$ ); **MB** (19.4 g NaCl, 8.8 g/L  $\text{MgCl}_2$ , 5 g/L peptone, 3.24 g/L  $\text{Na}_2\text{SO}_4$ , 1.8 g/L  $\text{CaCl}_2$ , 1 g/L yeast extract, 0.55 g/L KCl, 0.16 g/L  $\text{NaHCO}_3$ , 0.10 g/L Fe(III) citrate, 0.08 g/L KBr, 0.034 g/L  $\text{SrCl}_2$ , 0.022 g/L  $\text{H}_3\text{BO}_3$ , 0.008 g/L  $\text{Na}_2\text{HPO}_4$ , 0.004 g/L sodium-silicate, 0.0024 g/L NaF, 0.0016 g/L  $\text{NH}_4\text{NO}_3$ ); **TYP** (16 g/L bacto-tryptone, 16 g/L yeast extract, 10 g/L NaCl); **lysogeny broth (LB)** (10 g/L tryptone, 5 g/L yeast Extract, 10 g NaCl); **PPAS** (10 g/L peptone, 0.1 g/L  $\text{MgSO}_4$ , 1.09 g/L  $\text{NH}_4\text{Cl}$ , 1.5 g/L KCl, 18.9 g/L tris base, pH adjusted to 7.2 with HCl).

### 3.3. Extract Preparation

A single colony of a bacterial isolate was used to inoculate 3 mL of liquid MB or TYP media in a sterile bacteriological tube. After 48 h of incubation at 20 °C at 210 rpm, the pre-inoculum was used to inoculate 125 mL of the same medium in 500 mL flasks at an initial cell concentration of 0.01  $\text{OD}_{600}$ . The flasks were incubated up to 5 days at 20 °C at 210 rpm. The cultures were then centrifuged at  $6800 \times g$  at 4 °C for 45 min, the cell-free culture broths were collected and subjected to organic extraction twice with 2 volumes of ethyl acetate, in a 500 mL separatory funnel. The organic phase was collected and evaporated using a rotavapor (R-100, BUCHI, Flawil, Switzerland) and the extracts were weighted, dissolved in 100% DMSO at the concentration 100 mg/mL and stored at −20 °C.

M15 strain was also grown in PPAS supplemented with 12 different carbon sources at 1% *w/v* final concentration, such as glucose, mannose, rhamnose, starch, xylan, benzene, diesel, anthracene, pyrene, phenanthrene, glycerol, and UCO. After 5 days of incubation, 14 for PAHs, the cell-free culture broths were collected, and extractions were performed as described above.

### 3.4. Biosurfactant Screening

The presence of biosurfactants in the extracts was investigated by means of three tests, one carried out on 90 × 15 mm plate (CTAB agar plate method) and two in liquid (oil spreading test and emulsification capacity assays).

#### 3.4.1. CTAB Agar Method

The CTAB agar method, also called Blue agar, is an in-plate test that can reveal the presence of anionic biosurfactants by the arising of dark blue halos around the extracts. In this method, the anionic biosurfactants form an insoluble complex with cetyltrimethylammonium bromide, and the complex is revealed by the presence of methylene blue. Wells were made in the agar, with the wide top of a sterile Pasteur pipette, and filled with 8  $\mu\text{L}$  of the extracts, dissolved in DMSO at 100 mg/mL. As a negative control, 8  $\mu\text{L}$  of pure DMSO were used, while 8  $\mu\text{L}$  of 0.1% sodium dodecyl sulphate (SDS) were used as positive control. After 2 days at 4 °C, the extracts containing RLs were selected by the presence of a dark blue halo around the wells. The halo diameter was directly proportional to the surfactant concentration [2].

#### 3.4.2. Emulsification Capacity Assay

This test depends on the ability of biosurfactants to stabilize emulsions. The method was performed adding to 1 mL of n-hexane, 1 mL of free-cell culture supernatant in 6 mL glass tubes (7.5 cm × 1 cm) and vortexing for 2 min. Tween 20<sup>®</sup> (0.5% *v/v*) was used as positive control. After 24 h of incubation at room temperature, emulsification capacity was optically determined as a stable emulsion. Moreover, the E24 was calculated as the percentage of the height of the emulsified layer (mm) divided by the total height of the liquid column.

$$E24(\%) = \frac{\text{Emulsified layer height (mm)}}{\text{Total liquid height (mm)}} \times 100 \quad (1)$$

### 3.4.3. Oil-Spreading Test

The test was developed by Morikawa et al. [22] and can reveal the presence of biosurfactants by the solubilization of crude oil in water. In detail, biosurfactants can solubilize oil in water by micelles formation making a clear zone into the oil layer.

A thin oil layer on the water's surface was made adding 50  $\mu\text{L}$  of exhaust motor oil to 25 mL of distilled water in a Petri dish. Then, 1  $\mu\text{L}$  of crude extract at 1 mg/mL was delivered onto the oil. DMSO was used as a negative control.

### 3.5. Bacterial Identification

The identification of strains positive for both biosurfactant and antimicrobial screenings were carried out amplifying 16S rRNA gene using a single colony as template. PCR was carried out in a total volume of 50  $\mu\text{L}$ , containing 25  $\mu\text{L}$  of DreamTaq PCR Master Mix (a ready-to-use solution containing DreamTaq DNA Polymerase, optimized DreamTaq buffer,  $\text{MgCl}_2$ , and dNTPs), 0.2  $\mu\text{M}$  of both primer 27F (Forward, seq: 5'-AGAGTTTGATCCTGGCTCAG-3') and 1492R (Reverse, seq: 5'-GGTTACCTTGTTACGACTT-3'). The reaction conditions used were: one cycle (95 °C for 10 min), 30 cycles (95 °C for 30 s, 50 °C for 30 s, and 72 °C for 2 min), with a final extension of 7 min at 72 °C. PCR products were then purified by GenElute™ PCR Clean-UP kit (Sigma-Aldrich, Darmstadt, Germany), the purified PCR products were sequenced by Microgrem (Napoli, Italy). Both end sequences obtained by submitting the forward and the reverse to Prabi CAP3 [55] (<http://doua.prabi.fr/software/cap3>) were submitted to EzBioCloud for the affiliation analysis. Evolutionary analyses were conducted in MEGA X [56]. A phylogenetic tree was inferred using the neighbor-joining method [57]. The evolutionary distances were computed using the Kimura 2-parameter method [58] and were in the units of the number of base substitutions per site. All positions with less than 95% site coverage were eliminated, i.e., fewer than 5% alignment gaps, missing data, and ambiguous bases were allowed at any position (partial deletion option). Bootstrap values were calculated with 1000 resamples.

### 3.6. Biosurfactant Fraction Enrichment

The extract obtained from a 2 L culture of strain M15 in liquid TYP was re-suspended in the minimum possible amount of MeOH and subjected to fractionation using C18 cartridges (Macherey-Nagel, Duren, Germany), utilizing  $\text{H}_2\text{O}$ , MeOH and mixtures of the two in different percentages as eluents. Fractions eluted at 60%, 80% and 100% of MeOH were collected, dried and tested using the liquid antimicrobial assay and oil-displacement test.

### 3.7. Chemical Profiling and Structural Analysis of Biosurfactants

ESI-MS spectra were carried out in negative mode on a high-resolution mass spectrometer QToF Premiere (Waters Corp., Manchester, UK) equipped with Alliance 2610 pumps. The following parameters were set for MS: Capillary (kV) 3.2; Sampling Cone 40.0; Extraction Cone 3.0; Ion Guide 2.0, Collision Energy 5.0. The extracts were dissolved in MeOH at 12 mg/mL and 3  $\mu\text{L}$ , ca 20  $\mu\text{g}$ , were injected in a Kinetex reverse C18 column (Phenomenex, Torrance, CA, USA). The gradient was run at a flow of 200  $\mu\text{L}/\text{min}$ , using  $\text{H}_2\text{O}$  and MeOH, respectively, as solvent A and solvent B, and to both 5 mM ammonium acetate was added. The gradient went from 50% to 95% B in 45 min.

The MS/MS experiments, different carbon sources ESI-MS, and both TYP CE and fractions ESI-MS were conducted on a QTRAP 4500 (SCIEX, Framingham, MA, USA), with the ESI source in negative mode connected to a Nexera X2 UHPLC (Shimadzu, Kyoto, Japan), equipped with a ACQUITY UPLC BEH 2.1  $\times$  50 mm C18 column 1.7  $\mu\text{m}$  (Waters, Milford, MA, USA). The solvent system consists of mass grade solvents, (A) water containing 0.1% formic acid and (B) acetonitrile containing 0.1% formic acid. The gradient was programmed as follows: from 25% to 80% B in 60 min, from 80% to 100% in 1 min, 100% B isocratic for 7 min, from 100% to 25% B in 1 min and finally, the initial conditions were held for 3 min as a re-equilibration step. The flow rate was 0.2 mL/min, the injection volume was 3  $\mu\text{L}$ , and the

extracts were dissolved in MeOH at 10 mg/mL. The mass spectrometry conditions were as follows: source temperature 250 °C, capillary voltage −4.5 kV, range m/z 100–650. MS/MS conditions were as follows: collision energy at  $-35 \pm 15$  eV collision energy (CE) was used to fragment ions in the m/z 100–650 range.

The area of the RL peaks detected by LC-ESI-MS experiments carried out on QTRAP 4500 were obtained through the script “Manually Integrate” of Analyst® software (SCIEX, Framingham, MA, USA). Relative abundance of each peak was calculated as the percentage of the single RL peak divided by the sum of all the RLs peaks areas.

$$\text{Relative abundance} = \frac{\text{RL area}}{\text{Total RLs areas}} \times 100 \quad (2)$$

### 3.8. Antimicrobial Activity

The SPE fraction, enriched in RLs, were tested for their antimicrobial activity microtiter plates assay. The extracts were placed into each well of a 96-well microplate at an initial concentration of 200 µg/mL and serially 2-fold diluted using LB medium. A control for external contaminations was represented by wells containing only the medium. DMSO (2% v/v) was used as negative control to determine the effect of the solvent on bacterial growth. A single colony of each pathogen strain was used to inoculate 3 mL of liquid medium in a sterile 13 mL tube. After 5–8 h of incubation, growth was measured by monitoring the absorbance at 600 nm and about 40000 CFU were dispensed into each well of the prepared plate. Plates were incubated at 37 °C. The absorbance of the 96-well plates was measured at 600 nm at time zero and after an overnight growth, by ELX800 Absorbance Microplate Reader (Biotek, Winoosky, VT, USA), in order to evaluate the growth of the pathogens. To evaluate the antimicrobial capacity of the extracts, a panel of model multidrug resistant pathogens were used: *Acinetobacter baumannii* Ab13 [59], *Bacillus cereus* ATCC 14579 [60], *Burkholderia metallica* LMG 24068 [61], *K. pneumoniae* DF12SA [62], *E. coli* ATCC 10536 [63], *Listeria monocytogenes* MB 677 [64], *Pseudomonas aeruginosa* PA01 [65], *Salmonella enterica* serovar Enteritidis ATCC 13076 [66], *Salmonella enterica* serovar Typhimurium MB 4487 (ILVO), *Staphylococcus aureus* ATCC 29213 [67], *Staphylococcus aureus* 23235 [68], *Staphylococcus aureus* 6538P [69], *Staphylococcus epidermidis* ATCC 35984 [70], *Staphylococcus xylosus* MB 5209 [71], *Stenotrophomonas maltophilia* ATCC 13637 [72], *Stenotrophomonas maltophilia* ATCC 13636 [73] *Stenotrophomonas maltophilia* ATCC 700475 [74]. All pathogens were grown overnight in LB at 37 °C with orbital shaking at 210 rpm.

## 4. Conclusions

In this study, we isolated from Antarctic sediments a strain identified as *P. gessardii* and able to produce biosurfactants. LC-HRESMS analysis revealed the presence of 17 different mono-RLs in the extract. Structural analysis by LC-MS/MS revealed that six of them, Rha-C<sub>12:1</sub>-C<sub>8</sub>, Rha-C<sub>12:1</sub>-C<sub>12:1</sub>, Rha-C<sub>14:1</sub>-C<sub>12:1</sub>, Rha-C<sub>16:1</sub>-C<sub>10</sub>, Rha-C<sub>14:1</sub>-C<sub>12</sub>, and Rha-C<sub>12</sub>-C<sub>14:1</sub>, were never described before. We also investigated the ability of the strain to grow and produce RLs from cheap carbon sources and pollutants reporting the relative abundance of the singles RLs in each condition. The best results, in terms of relative abundance of the new RLs, were obtained from glycerol, oil, mannose and glucose. RL production obtained from diesel, benzene and anthracene was a remarkable result from a bioremediation point of view. Thus, M15 is able to use PAHs as a sole carbon source to grow and to produce RLs that help to degrade PAHs by the local microbial community. We also evaluated the antimicrobial potential of the whole RL mixtures, obtaining interesting results against *B. cereus*, *L. monocytogenes* and *S. aureus* and reporting for the first-time antimicrobial activity of RLs towards *S. maltophilia*. We also correlated the increments of the antimicrobial activity to Rha-C<sub>12:1</sub>-C<sub>12:1</sub>, Rha-C<sub>14:1</sub>-C<sub>10</sub> and Rha-C<sub>16:1</sub>-C<sub>10</sub>, through their relative abundance in the RL mixtures. Moreover, we highlighted the overproduction of the new RLs on glycerol and UCO, a finding that could be helpful in the future perspectives of isolation and purification of these compounds.

**Supplementary Materials:** The following are available online at <http://www.mdpi.com/1660-3397/18/5/269/s1>, Figure S1: HRESI-MS spectrum of compound 1, Figure S2: HRESI-MS spectrum of compound 2, Figure S3: HRESI-MS spectrum of compound 3, Figure S4: HRESI-MS spectrum of compound 4, Figure S5: HRESI-MS spectrum of compound 5, Figure S6: HRESI-MS spectrum of compound 6, Figure S7: HRESI-MS spectrum of compound 7, Figure S8: HRESI-MS spectrum of compound 8, Figure S9: HRESI-MS spectrum of compound 9, Figure S10: HRESI-MS spectrum of compound 10, Figure S11: HRESI-MS spectrum of compound 11, Figure S12: HRESI-MS spectrum of compound 12, Figure S13: HRESI-MS spectrum of compound 13, Figure S14: HRESI-MS spectrum of compound 14, Figure S15: HRESI-MS spectrum of compound 15, Figure S16: HRESI-MS spectrum of compound 16, Carbon source influence on RLs production, Figure S17: Base peak chromatogram of anthracene extract, Figure S18: Base Peak chromatogram of benzene extract, Figure S19: Base peak chromatogram of control extract, Figure S20: Base Peak chromatogram of diesel extract, Figure S21: Base peak chromatogram of glucose extract, Figure S22: Base Peak chromatogram of glycerol extract, Figure S23: Base peak chromatogram of mannose extract, Figure S24: Base Peak chromatogram of used cooking oil extract, Figure S25: Base peak chromatogram of phenanthrene extract, Figure S26: Base Peak chromatogram of pyrene extract Figure S27: Base peak chromatogram of rhamnose extract, Figure S28: Base peak chromatogram of starch extract, Figure S29: Base peak chromatogram of xylan extract.

**Author Contributions:** D.d.P., M.V.D. conceptualization; C.B., F.P.E., M.C.M., P.T., G.A.V., R.G., investigation and formal analysis; C.B., G.A.V., P.T., F.P.E. and M.V.D., wrote the manuscript. All authors read and corrected the manuscript. All authors have read and agreed to the published version of the manuscript.

**Funding:** This research was funded by H2020-MSCA-ITN-ETN MarPipe, grant number 721421 and by H2020-MSCA-RISE: Ocean Medicines grant number 690944.

**Conflicts of Interest:** The authors declare no conflict of interest.

## References

1. Soberón-Chávez, G.; Maier, R.M. Biosurfactants: A general overview. In *Biosurfactants: From Genes to Applications*; Soberón-Chávez, G., Ed.; Springer: Berlin, Germany, 2011; Volume 20, pp. 1–11.
2. Tiso, T.; Germer, A.; Küpper, B.; Wichmann, R.; Blank, L. *Methods for Recombinant Rhamnolipid Production*; Springer: Berlin, Germany, 2016. [[CrossRef](#)]
3. Abdel-Mawgoud, A.; Lépine, F.; Déziel, E. Rhamnolipids: Diversity of structures, microbial origins and roles. *Appl. Microbiol. Biotechnol.* **2010**, *86*, 1323–1336. [[CrossRef](#)] [[PubMed](#)]
4. Chen, J.; Wu, Q.; Hua, Y.; Chen, J.; Zhang, H.; Wang, H. Potential applications of biosurfactant rhamnolipids in agriculture and biomedicine. *App. Microbiol. Biotechnol.* **2017**, *101*, 8309–8319. [[CrossRef](#)] [[PubMed](#)]
5. Caiazza, N.C.; Shanks, R.M.; O’Toole, G.A. Rhamnolipids modulate swarming motility patterns of *Pseudomonas aeruginosa*. *J. Bacteriol.* **2005**, *187*, 7351–7361. [[CrossRef](#)] [[PubMed](#)]
6. Koch, A.K.; Kappeli, O.; Fiechter, A.; Reiser, J. Hydrocarbon assimilation and biosurfactant production in *Pseudomonas aeruginosa* mutants. *J. Bacteriol.* **1991**, *173*, 4212–4219. [[CrossRef](#)]
7. Davey, M.E.; Caiazza, N.C.; O’Toole, G.A. Rhamnolipid surfactant production affects biofilm architecture in *pseudomonas aeruginosa* PAO1. *J. Bacteriol.* **2003**, *185*, 1027–1036. [[CrossRef](#)]
8. Abalos, A.; Pinazo, A.; Infante, M.R.; Casals, M.; García, F.; Manresa, A. Physicochemical and antimicrobial properties of new rhamnolipids produced by *pseudomonas aeruginosa* AT10 from Soybean Oil Refinery Wastes. *Langmuir* **2001**, *17*, 1367–1371. [[CrossRef](#)]
9. Remichkova, M.; Galabova, D.; Roeva, I.; Karpenko, E.; Shulga, A.; Galabov, A.S. Anti-herpesvirus activities of *Pseudomonas* sp. S-17 rhamnolipid and its complex with alginate. *Z. Nat. C J. Biosci.* **2008**, *63*, 75–81. [[CrossRef](#)]
10. Wang, X.; Gong, L.; Liang, S.; Han, X.; Zhu, C.; Li, Y. Algicidal activity of rhamnolipid biosurfactants produced by *Pseudomonas aeruginosa*. *Harmful Algae* **2005**, *4*, 433–443. [[CrossRef](#)]
11. Goswami, D.; Borah, S.N.; Lahkar, J.; Handique, P.J.; Deka, S. Antifungal properties of rhamnolipid produced by *Pseudomonas aeruginosa* DS9 against *Colletotrichum falcatum*. *J. Basic Microbiol.* **2015**, *55*, 1265–1274. [[CrossRef](#)]
12. Mishra, A.; Dubey, R.; Yabaji, S.; Jaiswal, S. Evaluation of antimycobacterial rhamnolipid production from non-cytotoxic strains of *Pseudomonas aeruginosa* isolated from rhizospheric soil of medicinal plants. *Int. J. Biol. Res.* **2016**, *4*, 112. [[CrossRef](#)]
13. de Freitas Ferreira, J.; Vieira, E.A.; Nitschke, M. The antibacterial activity of rhamnolipid biosurfactant is pH dependent. *Food Res. Int.* **2019**, *116*, 737–744. [[CrossRef](#)] [[PubMed](#)]

14. Borah, S.N.; Goswami, D.; Sarma, H.K.; Cameotra, S.S.; Deka, S. Rhamnolipid biosurfactant against fusarium verticillioides to control stalk and ear rot disease of maize. *Front. Microbiol.* **2016**, *7*, 1505. [[CrossRef](#)] [[PubMed](#)]
15. Rampelotto, H.P. Polar microbiology: Recent advances and future perspectives. *Biology* **2014**, *3*, 81–84. [[CrossRef](#)]
16. Gudiña, E.J.; Teixeira, J.A.; Rodrigues, L.R. Biosurfactants produced by marine microorganisms with therapeutic applications. *Mar. Drugs* **2016**, *14*, 38. [[CrossRef](#)]
17. Perfumo, A.; Banat, I.M.; Marchant, R. Going green and cold: Biosurfactants from low-temperature environments to biotechnology applications. *Trends Biotechnol.* **2018**, *36*, 277–289. [[CrossRef](#)] [[PubMed](#)]
18. Tytgat, B.; Verleyen, E.; Obbels, D.; Peeters, K.; De Wever, A.; D'hondt, S.; De Meyer, T.; Van Crieckinge, W.; Vyverman, W.; Willems, A. Bacterial diversity assessment in antarctic terrestrial and aquatic microbial mats: A comparison between bidirectional pyrosequencing and cultivation. *PLoS ONE* **2014**, *9*, e97564. [[CrossRef](#)]
19. Wynn-Williams, D.D. Antarctic microbial diversity: The basis of polar ecosystem processes. *Biodivers. Conserv.* **1996**, *5*, 1271–1293. [[CrossRef](#)]
20. Tedesco, P.; Maida, I.; Palma Esposito, F.; Tortorella, E.; Subko, K.; Ezeofor, C.; Zhang, Y.; Tabudravu, J.; Jaspars, M.; Fani, R.; et al. Antimicrobial activity of monoramnolipids produced by bacterial strains isolated from the Ross Sea (Antarctica). *Mar. Drugs* **2016**, *14*, 83. [[CrossRef](#)]
21. Rahman, K.S.M.; Rahman, T.J.; McClean, S.; Marchant, R.; Banat, I.M. Rhamnolipid biosurfactant production by strains of pseudomonas aeruginosa using low-cost raw materials. *Biotechnol. Prog.* **2008**, *18*, 1277–1281. [[CrossRef](#)]
22. Morikawa, M.; Hirata, Y.; Imanaka, T. A study on the structure–function relationship of lipopeptide biosurfactants. *BBA Mol. Cell Biol. Lipids* **2000**, *1488*, 211–218. [[CrossRef](#)]
23. Siegmund, I.; Wagner, F. New method for detecting rhamnolipids excreted by Pseudomonas species during growth on mineral agar. *Biotechnol. Tech.* **1991**, *5*, 265–268. [[CrossRef](#)]
24. Walter, V.; Syldatk, C.; Hausmann, R. *Screening Concepts for the Isolation of Biosurfactant Producing Microorganisms*; Springer: New York, NY, USA, 2010; Volume 672, pp. 1–13. [[CrossRef](#)]
25. Yoon, S.H.; Ha, S.M.; Kwon, S.; Lim, J.; Kim, Y.; Seo, H.; Chun, J. Introducing EzBioCloud: A taxonomically united database of 16S rRNA gene sequences and whole-genome assemblies. *Int. J. Syst. Evol. Microbiol.* **2017**, *67*, 1613–1617. [[CrossRef](#)] [[PubMed](#)]
26. Verhille, S.; Baida, N.; Dabboussi, F.; Hamze, M.; Izard, D.; Leclerc, H. Pseudomonas gessardii sp. nov. and Pseudomonas migulae sp. nov., two new species isolated from natural mineral waters. *Int. J. Syst. Bacteriol.* **1999**, *49*, 1559–1572. [[CrossRef](#)]
27. Irorere, V.U.; Tripathi, L.; Marchant, R.; McClean, S.; Banat, I.M. Microbial rhamnolipid production: A critical re-evaluation of published data and suggested future publication criteria. *Appl. Microbiol. Biotechnol.* **2017**, *101*, 3941–3951. [[CrossRef](#)] [[PubMed](#)]
28. Kristoffersen, V.; Rämä, T.; Isaksson, J.; Andersen, H.J.; Gerwick, H.W.; Hansen, E. Characterization of rhamnolipids produced by an arctic marine bacterium from the pseudomonas fluorescence group. *Mar. Drugs* **2018**, *16*, 163. [[CrossRef](#)] [[PubMed](#)]
29. Hošková, M.; Schreiberová, O.; Ježdík, R.; Chudoba, J.; Masák, J.; Sigler, K.; Řezanka, T. Characterization of rhamnolipids produced by non-pathogenic Acinetobacter and Enterobacter bacteria. *Bioresour. Technol.* **2013**, *130*, 510–516. [[CrossRef](#)]
30. Řezanka, T.; Siristova, L.; Sigler, K. Rhamnolipid-producing thermophilic bacteria of species Thermus and Meiothermus. *Extremophiles* **2011**, *15*, 697. [[CrossRef](#)]
31. Sharma, A.; Jansen, R.; Nimtz, M.; Johri, B.N.; Wray, V. Rhamnolipids from the rhizosphere bacterium pseudomonas sp. GRP3 that reduces damping-off disease in chilli and tomato nurseries. *J. Nat. Prod.* **2007**, *70*, 941–947. [[CrossRef](#)]
32. Behrens, B.; Engelen, J.; Tiso, T.; Blank, L.M.; Hayen, H. Characterization of rhamnolipids by liquid chromatography/mass spectrometry after solid-phase extraction. *Anal. Bioanal. Chem.* **2016**, *408*, 2505–2514. [[CrossRef](#)]
33. Wittgens, A.; Santiago-Schuebel, B.; Henkel, M.; Tiso, T.; Blank, L.M.; Hausmann, R.; Hofmann, D.; Wilhelm, S.; Jaeger, K.-E.; Rosenau, F. Heterologous production of long-chain rhamnolipids from Burkholderia glumae in Pseudomonas putida—A step forward to tailor-made rhamnolipids. *Appl. Microbiol. Biotechnol.* **2018**, *102*, 1229–1239. [[CrossRef](#)]

34. Ramani, K.; Jain, S.C.; Mandal, A.B.; Sekaran, G. Microbial induced lipoprotein biosurfactant from slaughterhouse lipid waste and its application to the removal of metal ions from aqueous solution. *Colloids Surf. B* **2012**, *97*, 254–263. [[CrossRef](#)] [[PubMed](#)]
35. Díaz De Rienzo, M.A.; Kamalanathan, I.D.; Martin, P.J. Comparative study of the production of rhamnolipid biosurfactants by *B. thailandensis* E264 and *P. aeruginosa* ATCC 9027 using foam fractionation. *Process. Biochem.* **2016**, *51*, 820–827. [[CrossRef](#)]
36. Kumari, B.; Singh, S.N.; Singh, D.P. Characterization of two biosurfactant producing strains in crude oil degradation. *Process. Biochem.* **2012**, *47*, 2463–2471. [[CrossRef](#)]
37. Nicolò, M.S.; Cambria, M.G.; Impallomeni, G.; Rizzo, M.G.; Pellicorio, C.; Ballistreri, A.; Guglielmino, S.P.P. Carbon source effects on the mono/dirhamnolipid ratio produced by *Pseudomonas aeruginosa* L05, a new human respiratory isolate. *New Biotechnol.* **2017**, *39*, 36–41. [[CrossRef](#)]
38. Patowary, K.; Das, M.; Patowary, R.; Kalita, M.; Deka, S. Recycling of bakery waste as an alternative carbon source for rhamnolipid biosurfactant production. *J. Surfactants Deterg.* **2018**, 373–384. [[CrossRef](#)]
39. Tan, Y.N.; Li, Q. Microbial production of rhamnolipids using sugars as carbon sources. *Microb. Cell Fact.* **2018**, *17*, 89. [[CrossRef](#)]
40. Eraqi, W.A.; Yassin, A.S.; Ali, A.E.; Amin, M.A. Utilization of crude glycerol as a substrate for the production of rhamnolipid by *pseudomonas aeruginosa*. *Biotechnol. Res. Int.* **2016**, *2016*, 9. [[CrossRef](#)]
41. Chhetri, B.A.; Watts, C.K.; Islam, R.M. Waste cooking oil as an alternate feedstock for biodiesel production. *Energies* **2008**, *1*, 3–18. [[CrossRef](#)]
42. Singh, P.; Tiwary, B.N. Isolation and characterization of glycolipid biosurfactant produced by a *Pseudomonas otitidis* strain isolated from Chirimiri coal mines, India. *Bioresour. Bioprocess.* **2016**, *3*, 42. [[CrossRef](#)]
43. Abdel-Mawgoud, A.M.; Hausmann, R.; Lépine, F.; Müller, M.M.; Déziel, E. Rhamnolipids: Detection, analysis, biosynthesis, genetic regulation, and bioengineering of production. In *Biosurfactants: From Genes to Applications*; Soberón-Chávez, G., Ed.; Springer: Berlin/Heidelberg, Germany, 2011; pp. 13–55.
44. Abdel-Mawgoud, A.M.; Lépine, F.; Déziel, E. A stereospecific pathway diverts  $\beta$ -Oxidation intermediates to the biosynthesis of rhamnolipid biosurfactants. *Chem. Biol.* **2014**, *21*, 156–164. [[CrossRef](#)]
45. Peng, X.; Yuan, X.-Z.; Liu, H.; Zeng, G.-M.; Chen, X.-H. Degradation of polycyclic aromatic hydrocarbons (PAHs) by laccase in rhamnolipid reversed micellar system. *Appl. Biochem. Biotechnol.* **2015**, *176*, 45–55. [[CrossRef](#)]
46. Zhu, S.; Liang, S.; You, X. Effect of rhamnolipid biosurfactant on solubilization and biodegradation of polycyclic aromatic hydrocarbons. In Proceedings of the 2013 Third International Conference on Intelligent System Design and Engineering Applications, Hong Kong, China, 16–18 January 2013; pp. 651–654. [[CrossRef](#)]
47. Magalhães, L.; Nitschke, M. Antimicrobial activity of rhamnolipids against *Listeria monocytogenes* and their synergistic interaction with nisin. *Food Control* **2013**, *29*, 138–142. [[CrossRef](#)]
48. Onbasli, D.; Aslim, B. Determination of antimicrobial activity and production of some metabolites by *Pseudomonas aeruginosa* B1 and B2 in sugar beet molasses. *Afr. J. Biotechnol.* **2009**, *7*, 4614–4619.
49. Sotirova, A.V.; Spasova, D.I.; Galabova, D.N.; Karpenko, E.; Shulga, A. Rhamnolipid–biosurfactant permeabilizing effects on gram-positive and gram-negative bacterial strains. *Curr. Microbiol.* **2008**, *56*, 639–644. [[CrossRef](#)]
50. Das, P.; Yang, X.-P.; Ma, L.Z. Analysis of biosurfactants from industrially viable *Pseudomonas* strain isolated from crude oil suggests how rhamnolipids congeners affect emulsification property and antimicrobial activity. *Front. Microbiol.* **2014**, *5*, 696. [[CrossRef](#)]
51. Zhang, L.; Jiao, L.; Zhong, J.; Guan, W.; Lu, C. Light up the interactions between bacteria and surfactants with aggregation-induced emission characteristics. *Mater. Chem. Front.* **2017**, *1*, 1829–1835. [[CrossRef](#)]
52. Silhavy, T.J.; Kahne, D.; Walker, S. The bacterial cell envelope. *Cold Spring Harb. Perspect. Biol.* **2010**, *2*, a000414. [[CrossRef](#)]
53. Li, X.-Z.; Li, J. *Antimicrobial Resistance in Stenotrophomonas Maltophilia: Mechanisms and Clinical Implications*; Springer International: Cham, Switzerland, 2017; Volume 2, pp. 937–958. [[CrossRef](#)]
54. Looney, W.J.; Narita, M.; Mühlemann, K. *Stenotrophomonas maltophilia*: An emerging opportunist human pathogen. *Lancet Infect. Dis.* **2009**, *9*, 312–323. [[CrossRef](#)]
55. Huang, X.; Madan, A. CAP3: A DNA sequence assembly program. *Genome Res.* **1999**, *9*, 868–877. [[CrossRef](#)]
56. Kumar, S.; Stecher, G.; Li, M.; Nnyaz, C.; Tamura, K. MEGA X: Molecular evolutionary genetics analysis across computing platforms. *Mol. Biol. Evol.* **2018**, *35*, 1547–1549. [[CrossRef](#)]

57. Saitou, N.; Nei, M. The neighbor-joining method: A new method for reconstructing phylogenetic trees. *Mol. Biol. Evol.* **1987**, *4*, 406–425. [[CrossRef](#)] [[PubMed](#)]
58. Kimura, M. A simple method for estimating evolutionary rates of base substitutions through comparative studies of nucleotide sequences. *J. Mol. Evol.* **1980**, *16*, 111–120. [[CrossRef](#)] [[PubMed](#)]
59. Corvec, S.; Poirel, L.; Naas, T.; Drugeon, H.; Nordmann, P. Genetics and expression of the carbapenem-hydrolyzing oxacillinase gene blaOXA-23 in *Acinetobacter baumannii*. *Antimicrob. Agents Chemother.* **2007**, *51*, 1530–1533. [[CrossRef](#)] [[PubMed](#)]
60. Ivanova, N.; Sorokin, A.; Anderson, I.; Galleron, N.; Candelon, B.; Kapatral, V.; Bhattacharyya, A.; Reznik, G.; Mikhailova, N.; Lapidus, A.; et al. Genome sequence of *Bacillus cereus* and comparative analysis with *Bacillus anthracis*. *Nature* **2003**, *423*, 87–91. [[CrossRef](#)]
61. Soriano, F.; Huelves, L.; Naves, P.; Rodríguez-Cerrato, V.; del Prado, G.; Ruiz, V.; Ponte, C. In vitro activity of ciprofloxacin, moxifloxacin, vancomycin and erythromycin against planktonic and biofilm forms of *Corynebacterium urealyticum*. *J. Antimicrob. Chemother.* **2008**, *63*, 353–356. [[CrossRef](#)]
62. Shahi, S.K.; Kumar, A. Isolation and genetic analysis of multidrug resistant bacteria from diabetic foot ulcers. *Front. Microbiol.* **2016**, *6*, 1464. [[CrossRef](#)]
63. Alanazi, A.S.; Qureshi, K.A.; Elhassan, G.O.; Elsayed El-Agamy, E.I. Isolation, purification and characterization of antimicrobial agent antagonistic to *Escherichia coli* ATCC 10536 produced by *Bacillus pumilus* safr-032 isolated from the soil of Unaizah, Al-Qassim province of Saudi Arabia. *Pak. J. Biol. Sci.* **2016**, *19*, 191–201. [[CrossRef](#)]
64. Werbrouck, H.; Vermeulen, A.; Van Coillie, E.; Messens, W.; Herman, L.; Devlieghere, F.; Uyttendaele, M. Influence of acid stress on survival, expression of virulence genes and invasion capacity into Caco-2 cells of *Listeria monocytogenes* strains of different origins. *Int. J. Food Microbiol.* **2009**, *134*, 140–146. [[CrossRef](#)]
65. Stover, C.K.; Pham, X.Q.; Erwin, A.L.; Mizoguchi, S.D.; Warrener, P.; Hickey, M.J.; Brinkman, F.S.L.; Hufnagle, W.O.; Kowalik, D.J.; Lagrou, M.; et al. Complete genome sequence of *Pseudomonas aeruginosa* PAO1, an opportunistic pathogen. *Nature* **2000**, *406*, 959–964. [[CrossRef](#)]
66. Huang, C.; Virk, S.M.; Shi, J.; Zhou, Y.; Willias, S.P.; Morsy, M.K.; Abdelnabby, H.E.; Liu, J.; Wang, X.; Li, J. Isolation, characterization, and application of bacteriophage LPSE1 against *Salmonella enterica* in ready to eat (RTE) Foods. *Front. Microbiol.* **2018**, *9*, 1046. [[CrossRef](#)]
67. Azizkhani, M.; Misaghi, A.; Basti, A.A.; Gandomi, H.; Hosseini, H. Corrigendum to “effects of *Zataria multiflora* Boiss. essential oil on growth and gene expression of enterotoxins A, C and E in *Staphylococcus aureus* ATCC 29213.” [Int. J. Food Microbiol. 163 (2013) 159–165]. *Int. J. Food Microbiol.* **2013**, *166*, 125. [[CrossRef](#)]
68. Barry, A.L.; Jones, R.N. Criteria for disk susceptibility tests and quality control guidelines for the cefoperazone-sulbactam combination. *J. Clin. Microbiol.* **1988**, *26*, 13–17. [[CrossRef](#)]
69. Lima, D.B.; Torres, A.F.C.; Mello, C.P.; de Menezes, R.R.P.P.B.; Sampaio, T.L.; Canuto, J.A.; da Silva, J.J.A.; Freire, V.N.; Quinet, Y.P.; Havt, A.; et al. Antimicrobial effect of *Dinoponera quadricaps* (Hymenoptera: Formicidae) venom against *Staphylococcus aureus* strains. *J. Appl. Microbiol.* **2014**, *117*, 390–396. [[CrossRef](#)] [[PubMed](#)]
70. Gill, S.R.; Fouts, D.E.; Archer, G.L.; Mongodin, E.F.; Deboy, R.T.; Ravel, J.; Paulsen, I.T.; Kolonay, J.F.; Brinkac, L.; Beanan, M.; et al. Insights on evolution of virulence and resistance from the complete genome analysis of an early methicillin-resistant *Staphylococcus aureus* strain and a biofilm-producing methicillin-resistant *Staphylococcus epidermidis* strain. *J. Bacteriol.* **2005**, *187*, 2426–2438. [[CrossRef](#)] [[PubMed](#)]
71. Piessens, V.; De Vliegher, S.; Verbist, B.; Braem, G.; Van Nuffel, A.; De Vuyst, L.; Heyndrickx, M.; Van Coillie, E. Characterization of coagulase-negative staphylococcus species from cows’ milk and environment based on *bap*, *icaA*, and *mecA* genes and phenotypic susceptibility to antimicrobials and teat dips. *J. Dairy Sci.* **2012**, *95*, 7027–7038. [[CrossRef](#)] [[PubMed](#)]
72. Zhang, L.; Li, X.-Z.; Poole, K. Fluoroquinolone susceptibilities of efflux-mediated multidrug-resistant *Pseudomonas aeruginosa*, *Stenotrophomonas maltophilia* and *Burkholderia cepacia*. *J. Antimicrob. Chemother.* **2001**, *48*, 549–552. [[CrossRef](#)] [[PubMed](#)]

73. Huertas Méndez, N.D.J.; Vargas Casanova, Y.; Gómez Chimbi, A.K.; Hernández, E.; Leal Castro, A.L.; Melo Diaz, J.M.; Rivera Monroy, Z.J.; García Castañeda, J.E. Synthetic peptides derived from bovine lactoferricin exhibit antimicrobial activity against *E. coli* ATCC 11775, *S. maltophilia* ATCC 13636 and *S. enteritidis* ATCC 13076. *Molecules* **2017**, *22*, 452. [[CrossRef](#)]
74. Kaiser, S.; Biehler, K.; Jonas, D. A *Stenotrophomonas maltophilia* multilocus sequence typing scheme for inferring population structure. *J. Bacteriol.* **2009**, *191*, 2934–2943. [[CrossRef](#)]



© 2020 by the authors. Licensee MDPI, Basel, Switzerland. This article is an open access article distributed under the terms and conditions of the Creative Commons Attribution (CC BY) license (<http://creativecommons.org/licenses/by/4.0/>).